

---

# FedSKETCH: Communication-Efficient Federated Learning via Sketching

---

Anonymous Author(s)

Affiliation

Address

email

## Abstract

1       Communication complexity and data privacy are the two key challenges in Federated Learning (FL) where the goal is to perform a distributed learning through a  
2       large volume of devices. In this work, we introduce two new algorithms, namely  
3       FedSKETCH and FedSKETCHGATE, to address jointly both challenges and which  
4       are, respectively, intended to be used for homogeneous and heterogeneous data distribution settings. Our algorithms are based on a key and novel sketching technique,  
5       called HEAPRIX that is unbiased, compresses the accumulation of local gradients  
6       using count sketch, and exhibits communication-efficiency properties leveraging  
7       low-dimensional sketches. We provide sharp convergence guarantees of our  
8       algorithms and validate our theoretical findings with various sets of experiments.  
9  
10

## 1 Introduction

12       Federated Learning (FL) is a recently emerging framework for distributed large scale machine  
13       learning problems. In FL, data is distributed across devices [23, 33] and due to privacy concerns,  
14       users are only allowed to communicate with the parameter server. Formally, the optimization problem  
15       across  $p$  distributed devices is defined as follows:

$$\min_{\mathbf{x} \in \mathbb{R}^d, \sum_{j=1}^p q_j = 1} f(\mathbf{x}) \triangleq \sum_{j=1}^p q_j F_j(\mathbf{x}), \quad (1)$$

16       where  $F_j(\mathbf{x}) = \mathbb{E}_{\xi \in \mathcal{D}_j} [L_j(\mathbf{x}, \xi)]$  is the local cost function at device  $j$ ,  $q_j \triangleq \frac{n_j}{n}$ ,  $n_j$  is the number  
17       of data shards at device  $j$  and  $n = \sum_{j=1}^p n_j$  is the total number of data samples,  $\xi$  is a random  
18       variable distributed according to probability distribution  $\mathcal{D}_j$ , and  $L_j$  is a loss function that measures  
19       the performance of model  $\mathbf{x}$  at device  $j$ . We note that, while for the homogeneous setting we  
20       assume  $\{\mathcal{D}_j\}_{j=1}^p$  have the same distribution across devices and  $L_i = L_j$ ,  $1 \leq (i, j) \leq p$ , in the  
21       heterogeneous setting, these distributions and loss functions  $L_j$  can vary from a device to another.

22       There are several challenges that need to be addressed in FL in order to efficiently learn a global  
23       model that performs well in average for all devices:

24       – *Communication-efficiency*: There are often many devices communicating with the server, thus  
25       incurring immense communication overhead. One approach to reduce communication round is using  
26       *local SGD with periodic averaging* [48, 41, 47, 43] which periodically averages models after a few  
27       local updates, contrary to baseline SGD [6] where gradient averaging is performed at each iteration.  
28       Local SGD has been proposed in [33, 23] under the FL setting and its convergence analysis is studied  
29       in [41, 43, 48, 47], later on improved in the followup references [3, 12, 21, 39] for homogeneous  
30       setting. It is further extended to heterogeneous setting [12, 20, 46, 30, 38, 31]. The second approach to  
31       deal with communication cost aims at reducing the size of communicated message per communication  
32       round, such as local gradient quantization [1, 4, 42, 44, 45] or sparsification [2, 32, 40, 39].

33       – *Data heterogeneity*: Since locally generated data in each device may come from different distribution,  
34       local computations involved in FL setting can lead to poor convergence error in practice [27, 31].

To mitigate the negative impact of data heterogeneity, [13, 16, 31, 20] suggest applying variance reduction or gradient tracking techniques along local computations.

–*Privacy* [11, 14]: Privacy has been widely addressed by injecting an additional layer of randomness to respect differential-privacy property [34] or using cryptography-based approaches under secure multi-party computation [5]. Further study of challenges can be found in recent surveys [28] and [18].

To tackle the aforementioned challenges in FL jointly, sketching based algorithms [7, 9, 22, 25] are promising approaches. For instance, to reduce communication cost, [17] develops a distributed SGD algorithm using sketching along providing its convergence analysis in the homogeneous setting, and establish a communication complexity of order  $\mathcal{O}(\log(d))$  per round, where  $d$  is the dimension of the vector of parameters compared to  $\mathcal{O}(d)$  complexity per round of baseline mini-batch SGD. Yet, the proposed sketching scheme in [17], built from a communication-efficiency perspective, is based on a deterministic procedure which requires access to the exact information of the gradients, thus not meeting the privacy-preserving criteria. This systemic issue is partially addressed in [37].

Focusing on privacy, [26] derives a single framework in order to tackle these issues jointly and introduces `DiffSketch` algorithm, based on the Count Sketch operator, yet does not provide its convergence analysis. Additionally, the estimation error of `DiffSketch` is higher than the sketching scheme in [17] which may end up in poor convergence.

Our main contributions are summarized as follows:

- We provide a new algorithm – `HEAPRIX` – and theoretically show that it reduces the cost of communication between devices and server, based on unbiased sketching without requiring the broadcast of exact values of gradients to the server. Based on `HEAPRIX`, we develop general algorithms for communication-efficient and sketch-based FL, namely `FedSKETCH` and `FedSKETCHGATE` for homogeneous and heterogeneous data distribution settings respectively.
- We establish non-asymptotic convergence bounds for convex, Polyak-Łojasiewicz (PL) and non-convex functions in Theorems 1 and 2 in both homogeneous and heterogeneous cases, and highlight an improvement in the number of iteration to reach a stationary point. We also provide a convergence analysis for the `PRIVIX/DiffSketch`<sup>1</sup> algorithm proposed in [26].
- We illustrate the benefits of `FedSKETCH` and `FedSKETCHGATE` over baseline methods through a set of experiments. The latter shows the advantages of the `HEAPRIX` compression method achieving comparable test accuracy as Federated SGD (`FedSGD`) while compressing the information exchanged between devices and server.

**Notation:** We denote the number of communication rounds and bits per round and per device by  $R$  and  $B$  respectively. The count sketch of vector  $\mathbf{x}$  is designated by  $\mathbf{S}(\mathbf{x})$ .  $[p]$  denotes the set  $\{1, \dots, p\}$ .

## 2 Compression using Count Sketch

In this paper, we exploit the commonly used `Count Sketch` [7] which uses two sets of functions that encode any input vector  $\mathbf{x}$  into a hash table  $\mathbf{S}_{m \times t}(\mathbf{x})$ . Pairwise independent hash functions  $\{h_{j,1 \leq j \leq t} : [d] \rightarrow m\}$  are used along with another set of pairwise independent sign hash functions  $\{\text{sign}_{j,1 \leq j \leq t} : [d] \rightarrow \{+1, -1\}\}$  to map entries of  $\mathbf{x}$  ( $x_i$ ,  $1 \leq i \leq d$ ) into  $t$  different columns of  $\mathbf{S}_{m \times t}$ , wherein to lower the dimension of the input vector we usually have  $d \gg mt$ . The final update reads  $\mathbf{S}[j][h_j(i)] = \mathbf{S}[j][h_j(i)] + \text{sign}_j(i) \cdot x_i$  for any  $1 \leq j \leq t$ . There are various types of sketching algorithms which are developed based on count sketching that we develop in the following subsections. See the Appendix for the detailed Count Sketch algorithm.

### 2.1 Sketching based Unbiased Compressor

We define an unbiased compressor as follows:

**Definition 1** (Unbiased compressor). We call randomized function,  $C : \mathbb{R}^d \rightarrow \mathbb{R}^d$  an unbiased compression operator with  $\Delta \geq 1$ , if

$$\mathbb{E}[C(\mathbf{x})] = \mathbf{x} \quad \text{and} \quad \mathbb{E}[\|C(\mathbf{x})\|_2^2] \leq \Delta \|\mathbf{x}\|_2^2.$$

We denote this class of compressors by  $\mathbb{U}(\Delta)$ .

<sup>1</sup>We use `PRIVIX` and `DiffSketch` [26] interchangeably throughout the paper.

82 This definition leads to the following property

$$\mathbb{E} \left[ \|\mathbf{C}(\mathbf{x}) - \mathbf{x}\|_2^2 \right] \leq (\Delta - 1) \|\mathbf{x}\|_2^2 .$$

83 Note that if we let  $\Delta = 1$  then our algorithm reduces to the case of no compression. This property  
84 allows us to control the noise of the compression.

85 An instance of such unbiased compressor is PRIVIX which obtains an estimate of input  $\mathbf{x}$  from a  
86 count sketch noted  $\mathbf{S}(\mathbf{x})$ . In this algorithm, to query the quantity  $x_i$ , the  $i$ -th element of the vector  
87  $\mathbf{x}$ , we compute the median of  $t$  approximated values specified by the indices of  $h_j(i)$  for  $1 \leq j \leq t$ ,  
88 see [26], [which is introduced under the name of DiffSketch](#), or Algorithm 6 in the Appendix (for  
89 more details). For the purpose of our proof, we state the following crucial properties of the count  
90 sketch:

91 **Property 1** ([26]). *For any  $\mathbf{x} \in \mathbb{R}^d$ , we have:*

92 *Unbiased estimation: As in [26], we have  $\mathbb{E}_{\mathbf{S}} [\text{PRIVIX}[\mathbf{S}(\mathbf{x})]] = \mathbf{x}$ .*

93 *Bounded variance: For the given  $m < d$ ,  $t = \mathcal{O}(\ln(\frac{d}{\delta}))$  with probability  $1 - \delta$  we have:*

$$\mathbb{E}_{\mathbf{S}} \left[ \|\text{PRIVIX}[\mathbf{S}(\mathbf{x})] - \mathbf{x}\|_2^2 \right] \leq \frac{c \times d}{m} \|\mathbf{x}\|_2^2 ,$$

94 *where  $c$  ( $e \leq c < m$ ) is a positive constant independent of the dimension of the input,  $d$ .*

95 [We note that bounded variance assumption does not necessary implies any compression as  \$d\$  could](#)  
96 [be relatively large. Second, a version of this property is used in Section B of Appendix \[26\].](#) Thus,  
97 with probability  $1 - \delta$  we obtain  $\text{PRIVIX} \in \mathbb{U}(1 + c\frac{d}{m})$ .  $\Delta = 1 + c\frac{d}{m}$  implies that if  $m \rightarrow d$ , then  
98  $\Delta \rightarrow 1 + c$ , indicating a noisy reconstruction. The reference [26] shows that if the data is normally  
99 distributed, PRIVIX is differentially private [10], up to additional assumptions and algorithmic design.

## 100 2.2 Sketching based Biased Compressor

101 A biased compressor is defined as follows:

102 **Definition 2** (Biased compressor). *A (randomized) function,  $C : \mathbb{R}^d \rightarrow \mathbb{R}^d$  belongs to  $\mathbb{C}(\Delta, \alpha)$ , a*  
103 *class of compression operators with  $\alpha > 0$  and  $\Delta \geq 1$ , if*

$$\mathbb{E} \left[ \|\alpha \mathbf{x} - C(\mathbf{x})\|_2^2 \right] \leq \left( 1 - \frac{1}{\Delta} \right) \|\mathbf{x}\|_2^2 ,$$

104 The reference [15] proves that  $\mathbb{U}(\Delta) \subset \mathbb{C}(\Delta, \alpha)$ . An example of bi-  
105 ased compression via sketching and using  $\text{top}_m$  operation is given below:  
106

107 Following [17], HEAVYMIX with sketch size  
108  $\Theta(m \log(\frac{d}{\delta}))$  is a biased compressor with  
109  $\alpha = 1$  and  $\Delta = d/m$  with probability  $\geq 1 - \delta$ ,  
110 [meaning that it reconstruct the  \$\tilde{\mathbf{g}}\$  from input](#)  
111 [vector  \$\mathbf{g}\$ .](#) In other words, with probability  
112  $1 - \delta$ ,  $\text{HEAVYMIX} \in \mathbb{C}(\frac{d}{m}, 1)$ . We note  
113 that Algorithm 1 is a variation of the sketch-  
114 ing algorithm developed in [17] with distinc-  
115 tion that HEAVYMIX does not require a sec-  
116 ond round of communication to obtain the ex-  
117 act values of  $\text{top}_m$ . [This is mainly because in](#)  
118 [SKETCGED-SGD \[17\] server has to obtain the](#)  
119 [exact values of the average of sketches; however HEAVYMIX obtains exact value locally, thus does not](#)  
120 [require second round of communication.](#) Additionally, while a sketching algorithm implementing  
121 HEAVYMIX has smaller estimation error compared to PRIVIX, it requires having access to the exact  
122 values of  $\text{top}_m$ , therefore not benefiting from privacy properties contrary to PRIVIX. [In the following](#)  
123 [we introduce HEAPRIX which is built upon HEAVYMIX and PRIVIX methods.](#)

---

### Algorithm 1 HEAVYMIX

---

- 1: **Inputs:**  $\mathbf{S}(\mathbf{g})$ ; parameter  $m$
  - 2: Query the vector  $\tilde{\mathbf{g}} \in \mathbb{R}^d$  from  $\mathbf{S}(\mathbf{g})$ :
  - 3: Query  $\hat{\ell}_2^2 = (1 \pm 0.5) \|\mathbf{g}\|^2$  from sketch  $\mathbf{S}(\mathbf{g})$
  - 4:  $\forall j$  query  $\hat{\mathbf{g}}_j^2 = \hat{\mathbf{g}}_j^2 \pm \frac{1}{2m} \|\mathbf{g}\|^2$  from sketch  $\mathbf{S}(\mathbf{g})$
  - 5:  $H = \{j | \hat{\mathbf{g}}_j \geq \frac{\hat{\ell}_2^2}{m}\}$  and  $NH = \{j | \hat{\mathbf{g}}_j < \frac{\hat{\ell}_2^2}{m}\}$
  - 6:  $\text{Top}_m = H \cup \text{rand}_{\ell}(NH)$ , where  $\ell = m - |H|$
  - 7: Get exact values of  $\text{Top}_m$
  - 8: **Output:**  $\tilde{\mathbf{g}} : \forall j \in \text{Top}_m : \tilde{\mathbf{g}}_i = \mathbf{g}_i$  else  $\mathbf{g}_i = 0$
-

## 2.3 Sketching based Induced Compressor

Due to Theorem 3 in [15], which illustrates that we can convert the biased compressor into an unbiased one such that, for  $C_1 \in \mathbb{C}(\Delta_1)$  with  $\alpha = 1$ , if you choose  $C_2 \in \mathbb{U}(\Delta_2)$ , then induced compressor  $C : x \mapsto C_1(x) + C_2(x - C_1(x))$  belongs to  $\mathbb{U}(\Delta)$  with  $\Delta = \Delta_2 + \frac{1-\Delta_2}{\Delta_1}$ .

Based on this notion, Algorithm 2 proposes an induced sketching algorithm by utilizing HEAVYMIX and PRIVIX for  $C_1$  and  $C_2$  respectively where the reconstruction of input  $x$  is performed using hash table  $S$  and  $x$ , similar to PRIVIX and HEAVYMIX. Note that if  $m \rightarrow d$ , then  $C(x) \rightarrow x$ , implying that the convergence rate can be improved by decreasing the size of compression  $m$ .

---

### Algorithm 2 HEAPRIX

---

- 1: **Inputs:**  $x \in \mathbb{R}^d, t, m, S_{m \times t}, h_j (1 \leq i \leq t), \text{sign}_j (1 \leq i \leq t)$ , parameter  $m$
  - 2: Approximate  $S(x)$  using HEAVYMIX
  - 3: Approximate  $S(x - \text{HEAVYMIX}[S(x)])$  with PRIVIX
  - 4: **Output:**  
 $\text{HEAVYMIX}[S(x)] + \text{PRIVIX}[S(x - \text{HEAVYMIX}[S(x)])]$
- 

**Corollary 1.** Based on Theorem 3 of [15], HEAPRIX in Algorithm 2 satisfies  $C(x) \in \mathbb{U}(c \frac{d}{m})$ .

*Benefits of HEAPRIX:* Corollary 1 states that, unlike PRIVIX, HEAPRIX compression noise can be made as small as possible using larger hash size. In the distributed setting, contrary to SKETCHED-SGD [17] where decompressing is happening at the server, HEAPRIX does not require having access to exact  $\text{top}_m$  values of the input as it is based on HEAVYMIX, thus helps preserving privacy. In other words, HEAPRIX leverages the best of both: the unbiasedness of PRIVIX while using heavy hitters as in HEAVYMIX.

## 3 FedSKETCH and FedSKETCHGATE

We introduce two new algorithms for both homogeneous and heterogeneous settings.

### 3.1 Homogeneous Setting

In FedSKETCH, the number of local updates, between two consecutive communication rounds, at device  $j$  is denoted by  $\tau$ . Unlike [13], server node does not store any global model, rather, device  $j$  has two models:  $x_j^{(r)}$  and  $x_j^{(\ell, r)}$ , which are respectively the local and global models. We develop FedSKETCH in Algorithm 3. A variant of this algorithm implementing HEAPRIX is also described in Algorithm 3. We remark that for this variant, we need to have an additional communication round between server and worker  $j$  to aggregate  $\delta_j^{(r)} \triangleq S_j[\text{HEAVYMIX}(S^{(r)})]$  (Lines 3 and 3) to construct  $S^{(r)} = \frac{1}{k} \sum_{j \in \mathcal{K}} S_j^{(r)}$ . The main difference between FedSKETCH and DiffSketch in [26] is that we use distinct local and global learning rates. Furthermore, unlike [26], we do not add local Gaussian noise.

**Algorithmic comparison with [13]** An important feature of our algorithm is that due to a lower dimension of the count sketch, the resulting averages ( $S^{(r)}$  and  $\tilde{S}^{(r)}$ ) received by the server, are also of lower dimension. Therefore, these algorithms exploit a bidirectional compression

---

### Algorithm 3 FedSKETCH( $R, \tau, \eta, \gamma$ )

---

- 1: **Inputs:**  $x^{(0)}$ : initial model shared by local devices, global and local learning rates  $\gamma$  and  $\eta$ , respectively
  - 2: **for**  $r = 0, \dots, R - 1$  **do**
  - 3: **parallel for device**  $j \in \mathcal{K}^{(r)}$  **do:**
  - 4: **if PRIVIX variant:**  
 $\Phi^{(r)} \triangleq \text{PRIVIX}[S^{(r-1)}]$
  - 5: **if HEAPRIX variant:**  
 $\Phi^{(r)} \triangleq \text{HEAVYMIX}[S^{(r-1)}] + \text{PRIVIX}[S^{(r-1)} - \tilde{S}^{(r-1)}]$
  - 6: Set  $x_j^{(r)} = x_j^{(r-1)} - \gamma \Phi^{(r)}$  and  $x_j^{(0, r)} = x_j^{(r)}$
  - 7: **for**  $\ell = 0, \dots, \tau - 1$  **do**
  - 8: Sample a mini-batch  $\xi_j^{(\ell, r)}$  and compute  $\tilde{g}_j^{(\ell, r)}$
  - 9: Update  $x_j^{(\ell+1, r)} = x_j^{(\ell, r)} - \eta \tilde{g}_j^{(\ell, r)}$
  - 10: **end for**
  - 11: Device  $j$  broadcasts  $S_j^{(r)} \triangleq S_j(x_j^{(0, r)} - x_j^{(\tau, r)})$ .
  - 12: Server computes  $S^{(r)} = \frac{1}{k} \sum_{j \in \mathcal{K}} S_j^{(r)}$ .
  - 13: Server broadcasts  $S^{(r)}$  to devices in randomly drawn devices  $\mathcal{K}^{(r)}$ .
  - 14: **if HEAPRIX variant:**
  - 15: Second round of communication:  $\delta_j^{(r)} \triangleq S_j[\text{HEAVYMIX}(S^{(r)})]$  and broadcasts  $\tilde{S}^{(r)} \triangleq \frac{1}{k} \sum_{j \in \mathcal{K}} \delta_j^{(r)}$  to devices in set  $\mathcal{K}^{(r)}$
  - 16: **end parallel for**
  - 17: **end**
  - 18: **Output:**  $x^{(R-1)}$
-

176 during the communication from server to device back and forth. As a result, due to this bidirectional  
 177 property of communicating sketching for the case of large quantization error  $\omega = \theta(\frac{d}{m})$  as shown  
 178 in [13], our algorithms can outperform FedCOM and FedCOMGATE developed in [13] if sufficiently  
 179 large hash tables are used and the uplink communication cost is high. Furthermore, while, in [13],  
 180 server stores a global model and aggregates the partial gradients from devices which can enable the  
 181 server to extract some information regarding the device's data, in contrast, in our algorithms server  
 182 does not store the global model and only broadcasts the average sketches. Thus, sketching-based  
 183 server-devices communication algorithms such as ours do not reveal the exact values of the inputs, to  
 184 preserve privacy as a by-product.

185 **Remark 1.** As pointed out in [15], while induced compressors transform a biased compressor into  
 186 unbiased one, as a drawback it doubles communication cost since the devices need to send  $C_1(\mathbf{x})$  and  
 187  $C_2(\mathbf{x} - C_1(\mathbf{x}))$  separately. We note that in the special case of HEAPRIX, due to the use of sketching,  
 188 the extra communication round cost is compensated with lower number of bits per round thanks to  
 189 the lower dimension of sketching.

### 190 3.2 Heterogeneous Setting

191 In this section, we focus on the optimiza-  
 192 tion problem of (1) in the special case  
 193 of  $q_1 = \dots = q_p = \frac{1}{p}$  with full de-  
 194 vice participation ( $k = p$ ). These results  
 195 can be extended to the scenario where de-  
 196 vices are sampled. For non i.i.d. data, the  
 197 FedSKETCH algorithm, designed for homo-  
 198 geneous setting, may fail to perform well  
 199 in practice. The main reason is that in  
 200 FL, devices are using local stochastic de-  
 201 scent direction which could be different  
 202 than global descent direction when the data  
 203 distribution are non-identical. Therefore,  
 204 to mitigate the effect of data heterogene-  
 205 ity, we introduce a new algorithm called  
 206 FedSKETCHGATE described in Algorithm 4.  
 207 This algorithm leverages the idea of gra-  
 208 dient tracking applied in [13] (with com-  
 209 pression) and a special case of  $\gamma = 1$  with-  
 210 out compression [31]. The main idea is  
 211 that using an approximation of global gra-  
 212 dient,  $\mathbf{c}_j^{(r)}$  allows to correct the local gra-  
 213 dient direction. For the FedSKETCHGATE  
 214 with PRIVIX variant, the correction vec-  
 215 tor  $\mathbf{c}_j^{(r)}$  at device  $j$  and communication  
 216 round  $r$  is computed in Line 4. While using  
 217 HEAPRIX compression, FedSKETCHGATE  
 218 also updates  $\tilde{\mathbf{S}}^{(r)}$  via Line 4.

219 **Remark 2.** Most of the existing  
 220 communication-efficient algorithms with  
 221 compression only consider communication-  
 222 efficiency from devices to server. However,  
 223 Algorithms 3 and 4 also improve the communication efficiency from server to devices since it exploits  
 224 low-dimensional sketches (and averages), communicated from the server to devices.

225 For both FedSKETCH and FedSKETCHGATE algorithms, unlike PRIVIX, HEAPRIX variant requires  
 226 a second round of communication. Therefore, in Cross-Device FL setting, where there could be  
 227 millions of devices, HEAPRIX variant may not be practical, and we note that it could be more suitable  
 228 for Cross-Silo FL setting.

---

#### Algorithm 4 FedSKETCHGATE( $R, \tau, \eta, \gamma$ )

---

1: **Inputs:**  $\mathbf{x}^{(0)} = \mathbf{x}_j^{(0)}$  shared by all local devices,  
 global and local learning rates  $\gamma$  and  $\eta$ .  
 2: **for**  $r = 0, \dots, R - 1$  **do**  
 3: **parallel for device**  $j = 1, \dots, p$  **do:**  
 4: **if PRIVIX variant:**  

$$\mathbf{c}_j^{(r)} = \mathbf{c}_j^{(r-1)} - \frac{1}{\tau} \left[ \text{PRIVIX}(\mathbf{S}^{(r-1)}) - \text{PRIVIX}(\mathbf{S}_j^{(r-1)}) \right]$$
  
 where  $\Phi^{(r)} \triangleq \text{PRIVIX}(\mathbf{S}^{(r-1)})$   
 5: **if HEAPRIX variant:**  

$$\mathbf{c}_j^{(r)} = \mathbf{c}_j^{(r-1)} - \frac{1}{\tau} (\Phi^{(r)} - \Phi_j^{(r)})$$
  
 6: Set  $\mathbf{x}^{(r)} = \mathbf{x}^{(r-1)} - \gamma \Phi^{(r)}$  and  $\mathbf{x}_j^{(0,r)} = \mathbf{x}^{(r)}$   
 7: **for**  $\ell = 0, \dots, \tau - 1$  **do**  
 8: Sample mini-batch  $\xi_j^{(\ell,r)}$  and compute  $\tilde{\mathbf{g}}_j^{(\ell,r)}$   
 9:  $\mathbf{x}_j^{(\ell+1,r)} = \mathbf{x}_j^{(\ell,r)} - \eta (\tilde{\mathbf{g}}_j^{(\ell,r)} - \mathbf{c}_j^{(r)})$   
 10: **end for**  
 11: Device  $j$  broadcasts  $\mathbf{S}_j^{(r)} \triangleq \mathbf{S}(\mathbf{x}_j^{(0,r)} - \mathbf{x}_j^{(\tau,r)})$ .  
 12: Server **computes**  $\mathbf{S}^{(r)} = \frac{1}{p} \sum_{j=1}^p \mathbf{S}_j^{(r)}$  and **broad-**  
**casts**  $\mathbf{S}^{(r)}$  to all devices.  
 13: **if HEAPRIX variant:**  
 14: Device  $j$  computes  $\Phi_j^{(r)} \triangleq \text{HEAPRIX}[\mathbf{S}_j^{(r)}]$   
 15: Second round of communication to obtain  $\delta_j^{(r)} :=$   
 $\mathbf{S}_j(\text{HEAVYMIX}[\mathbf{S}^{(r)}])$   
 16: Broadcasts  $\tilde{\mathbf{S}}^{(r)} \triangleq \frac{1}{p} \sum_{j=1}^p \delta_j^{(r)}$  to devices  
 17: **end parallel for**  
 18: **end**  
 19: **Output:**  $\mathbf{x}^{(R-1)}$

---

## 4 Convergence Analysis

We first state commonly used assumptions required in the following convergence analysis (reminder of our notations can be found Table 1 of the Appendix).

**Assumption 1** (Smoothness and Lower Boundedness). *The local objective function  $f_j(\cdot)$  of device  $j$  is differentiable for  $j \in [p]$  and  $L$ -smooth, i.e.,  $\|\nabla f_j(\mathbf{x}) - \nabla f_j(\mathbf{y})\| \leq L\|\mathbf{x} - \mathbf{y}\|$ ,  $\forall \mathbf{x}, \mathbf{y} \in \mathbb{R}^d$ . Moreover, the optimal objective function  $f(\cdot)$  is bounded below by  $f^* := \min_{\mathbf{x}} f(\mathbf{x}) > -\infty$ .*

Assumption 1 is common in stochastic optimization. We present our results for PL, convex and general non-convex objectives. [19] show that PL condition implies strong convexity property with same module (PL objectives can also be non-convex, hence strong convexity does not imply PL condition necessarily).

### 4.1 Convergence of FEDSKETCH

We now focus on the homogeneous case where data is i.i.d. among local devices, and therefore, the stochastic local gradient of each worker is an unbiased estimator of the global gradient. We have:

**Assumption 2** (Bounded Variance). *For all  $j \in [m]$ , we can sample an independent mini-batch  $\ell_j$  of size  $|\Xi_j^{(\ell, r)}| = b$  and compute an unbiased stochastic gradient  $\tilde{\mathbf{g}}_j = \nabla f_j(\mathbf{x}; \Xi_j)$ ,  $\mathbb{E}_{\Xi_j}[\tilde{\mathbf{g}}_j] = \nabla f(\mathbf{x}) = \mathbf{g}$  with the variance bounded is bounded by a constant  $\sigma^2$ , i.e.,  $\mathbb{E}_{\Xi_j}[\|\tilde{\mathbf{g}}_j - \mathbf{g}\|^2] \leq \sigma^2$ .*

**Theorem 1.** *Suppose Assumptions 1-2 hold. Given  $0 < m \leq d$  and considering Algorithm 3 with sketch size  $B = O(m \log(\frac{dR}{\delta}))$  and  $\gamma \geq k$ , with probability  $1 - \delta$  we have:*

*In the **non-convex** case,  $\{\mathbf{x}^{(r)}\}_{r=0}^R$  satisfies  $\frac{1}{R} \sum_{r=0}^{R-1} \mathbb{E}[\|\nabla f(\mathbf{x}^{(r)})\|_2^2] \leq \epsilon$  if:*

• **FS-PRIVIX**, for  $\eta = \frac{1}{L\gamma} \sqrt{\frac{k}{R\tau(\frac{cd}{mk} + 1)}}$ :  $R = O(1/\epsilon)$  and  $\tau = O((d+m)/(mk\epsilon))$ .

• **FS-HEAPRIX**, for  $\eta = \frac{1}{L\gamma} \sqrt{\frac{k}{R\tau(\frac{cd-m}{mk} + 1)}}$ :  $R = O(1/\epsilon)$  and  $\tau = O(d/(mk\epsilon))$ .

*In the **PL or strongly convex** case,  $\{\mathbf{x}^{(r)}\}_{r=0}^R$  satisfies  $\mathbb{E}[f(\mathbf{x}^{(R-1)}) - f(\mathbf{x}^{(*)})] \leq \epsilon$  if we set:*

• **FS-PRIVIX**, for  $\eta = \frac{1}{2L(cd/mk+1)\tau\gamma}$ :  $R = O((d/mk+1)\kappa \log(1/\epsilon))$  and  $\tau = O((d/m+1)/(d/m+k)\epsilon)$ .

• **FS-HEAPRIX**, for  $\eta = \frac{1}{2L((cd-m)/mk+1)\tau\gamma}$ :  $R = O(((d-m)/mk+1)\kappa \log(1/\epsilon))$  and  $\tau = O(d/m/((d/m-1)+k)\epsilon)$ .

*In the **Convex** case,  $\{\mathbf{x}^{(r)}\}_{r=0}^R$  satisfies  $\mathbb{E}[f(\mathbf{x}^{(R-1)}) - f(\mathbf{x}^{(*)})] \leq \epsilon$  if we set:*

• **FS-PRIVIX**, for  $\eta = \frac{1}{2L(cd/mk+1)\tau\gamma}$ :  $R = O(L(1+d/mk)/\epsilon \log(1/\epsilon))$  and  $\tau = O((d/m+1)^2/(k(d/mk+1)^2\epsilon^2))$ .

• **FS-HEAPRIX**, for  $\eta = \frac{1}{2L((cd-m)/mk+1)\tau\gamma}$ :  $R = O(L(1+(d-m)/mk)/\epsilon \log(1/\epsilon))$  and  $\tau = O((d/m)^2/(k([d-m]/mk+1)^2\epsilon^2))$ .

The bounds in Theorem 1 suggest that in homogeneous setting if we set  $d = m$  (no compression), the number of communication rounds to achieve the  $\epsilon$  error matches with the number of iterations required to achieve the same error under a centralized setting. Additionally, computational complexity scales down with number of sampled devices. To stress on the further impact of using sketching, we also compare our results with prior works in terms of total number of communicated bits per device.

**Comparison with [17]** From privacy aspect, we note [17] requires for server to have access to exact values of top<sub>m</sub> gradients, hence do not preserve privacy, whereas our schemes do not need those exact values. From communication cost point of view, for strongly convex objective and compared to [17],

we improve the total communication per worker from  $RB = O\left(\frac{d}{\epsilon} \log\left(\frac{d}{\delta\sqrt{\epsilon}} \max\left(\frac{d}{m}, \frac{1}{\sqrt{\epsilon}}\right)\right)\right)$  to

$$RB = O\left(\kappa\left(\frac{d-m}{k} + m\right) \log \frac{1}{\epsilon} \log\left(\frac{\kappa d}{\delta}\left(\frac{d-m}{mk} + 1\right) \log \frac{1}{\epsilon}\right)\right).$$

We note that while reducing communication cost, our scheme requires  $\tau = O(d/m(k(\frac{d}{mk}+1)\epsilon)) > 1$ , which scales down with the number of sampled devices,  $k$ . Moreover, unlike [17], we do not use bounded gradient assumption. Therefore, we obtain stronger result with weaker assumptions. Regarding general non-convex objectives, our result improves the total communication cost per worker in [17] from  $RB = O\left(\max(\frac{1}{\epsilon^2}, \frac{d^2}{k^2\epsilon}) \log(\frac{d}{\delta} \max(\frac{1}{\epsilon^2}, \frac{d^2}{k^2\epsilon}))\right)$  for *only one device* to  $RB = O(\frac{m}{\epsilon} \log(\frac{d}{\epsilon\delta}))$ . We also highlight that we can obtain similar rates for Algorithm 3 in heterogeneous environment if we make the additional assumption of uniformly bounded gradient.

**Note:** Such improved communication cost over prior related works is due to joint exploitation of *sketching*, to reduce the dimension of communicated messages, and the use of *local updates*, to reduce the total number of communication rounds leading to a specific convergence error.

## 4.2 Convergence of FedSKETCHGATE

We start with bounded local variance assumption:

**Assumption 3** (Bounded Local Variance). *For all  $j \in [p]$ , we can sample an independent mini-batch  $\Xi_j$  of size  $|\xi_j| = b$  and compute an unbiased stochastic gradient  $\tilde{\mathbf{g}}_j = \nabla f_j(\mathbf{x}; \Xi_j)$  with  $\mathbb{E}_{\Xi}[\tilde{\mathbf{g}}_j] = \nabla f_j(\mathbf{x}) = \mathbf{g}_j$ . Moreover, the variance of local stochastic gradients is bounded such that  $\mathbb{E}_{\Xi}[\|\tilde{\mathbf{g}}_j - \mathbf{g}_j\|^2] \leq \sigma^2$ .*

**Theorem 2.** *Suppose Assumptions 1 and 3 hold. Given  $0 < m \leq d$ , and considering FedSKETCHGATE in Algorithm 4 with sketch size  $B = O(m \log(\frac{dR}{\delta}))$  and  $\gamma \geq p$  with probability  $1 - \delta$  we have*

*In the **non-convex** case,  $\eta = \frac{1}{L\gamma} \sqrt{\frac{mp}{R\tau(cd)}}$ ,  $\{\mathbf{x}^{(r)}\}_{r=0}^{\infty}$  satisfies  $\frac{1}{R} \sum_{r=0}^{R-1} \mathbb{E}[\|\nabla f(\mathbf{x}^{(r)})\|_2^2] \leq \epsilon$  if:*

• **FS-PRIVIX:**

$$R = O((d+m)/m\epsilon) \quad \text{and} \quad \tau = O(1/(p\epsilon)).$$

• **FS-HEAPRIX:**  $R = O(d/m\epsilon)$  and  $\tau = O(1/(p\epsilon))$ .

*In the **PL or Strongly convex** case,  $\{\mathbf{x}^{(r)}\}_{r=0}^{\infty}$  satisfies  $\mathbb{E}[f(\mathbf{x}^{(R-1)}) - f(\mathbf{x}^{(*)})] \leq \epsilon$  if:*

• **FS-PRIVIX**, for  $\eta = 1/(2L(\frac{cd}{m} + 1)\tau\gamma)$ :  $R = O((\frac{d}{m} + 1)\kappa \log(1/\epsilon))$  and  $\tau = O(1/(p\epsilon))$

• **FS-HEAPRIX**, for  $\eta = m/(2cLd\tau\gamma)$ :  $R = O((\frac{d}{m})\kappa \log(1/\epsilon))$  and  $\tau = O(1/(p\epsilon))$ .

*In the **convex** case,  $\{\mathbf{x}^{(r)}\}_{r=0}^{\infty}$  satisfies  $\mathbb{E}[f(\mathbf{x}^{(R-1)}) - f(\mathbf{x}^{(*)})] \leq \epsilon$  if:*

• **FS-PRIVIX**, for  $\eta = 1/(2L(cd/m + 1)\tau\gamma)$ :  $R = O(L(d/m + 1)\epsilon \log(1/\epsilon))$  and  $\tau = O(1/(p\epsilon^2))$ .

• **FS-HEAPRIX**, for  $\eta = m/(2Lcd\tau\gamma)$ :  $R = O(L(d/m)\epsilon \log(1/\epsilon))$  and  $\tau = O(1/(p\epsilon^2))$ .

Theorem 2 implies that the number of communication rounds and local updates are similar to the corresponding quantities in homogeneous setting except for the non-convex case where the number of communication rounds also depends on the compression rate.

These results are summarized in Table 2-3 of the Appendix.

## 4.3 Comparison with Prior Methods

Before comparing with prior works, we highlight that privacy is another purpose of using unbiased sketching in addition to communication efficiency. Therefore, our main competing schemes are distributed algorithms based on sketching. Nonetheless, for the sake of showing the effectiveness of our algorithms, we also compare with prior non-sketching based distributed algorithms ([20, 3, 36, 13]) in Section B of Appendix.

**Comparison with [26].** Note that our convergence analysis does not rely on the bounded gradient assumption. We also improve both the number of communication rounds  $R$  and the size of transmitted



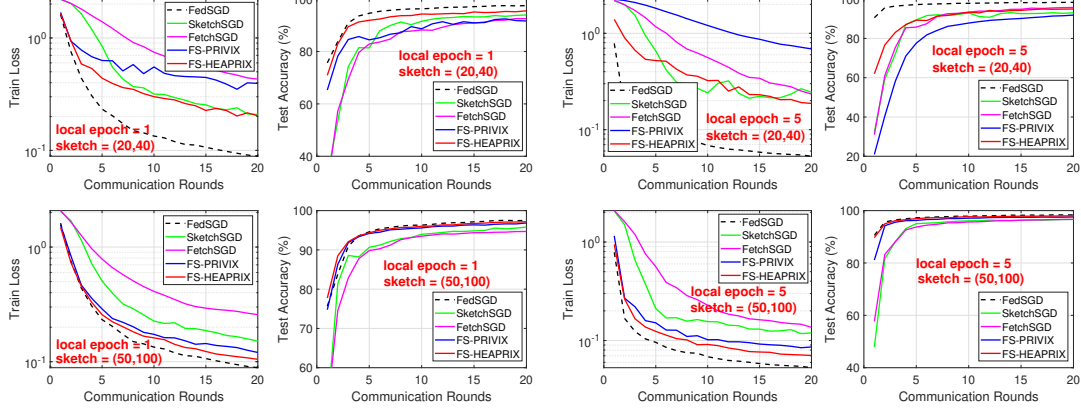


Figure 1: Homogeneous case: Comparison of compressed optimization methods on LeNet CNN.

bits  $B$  per communication round. Additionally, we highlight that, while [26] provides a convergence analysis for convex objectives, our analysis holds for PL (thus strongly convex case), general convex and general non-convex objectives.

**Comparison with [37].** Due to gradient tracking, our algorithm tackles data heterogeneity issue, while algorithms in [37] does not particularly. As a consequence, in FedSKETCHGATE each device has to store an additional state vector compared to [37]. Yet, as our method is built upon an unbiased compressor, server does not need to store any additional error correction vector. The convergence results for both of two variants of FetchSGD in [37] rely on the uniform bounded gradient assumption which may not be applicable with  $L$ -smoothness assumption when data distribution is highly heterogeneous, as in FL, see [21], while our bounds do not assume such boundedness. Besides, Theorem 1 [37] assumes that *Contraction Holds* for the sequence of gradients which may not hold in practice, yet based on this strong assumption, their total communication cost ( $RB$ ) in order to achieve  $\epsilon$  error is  $RB = O\left(m \max\left(\frac{1}{\epsilon^2}, \frac{d^2 - dm}{m^2 \epsilon}\right) \log\left(\frac{d}{\delta} \max\left(\frac{1}{\epsilon^2}, \frac{d^2 - dm}{m^2 \epsilon}\right)\right)\right)$ . For the sake of comparison we let the compression ratio in [37] to be  $\frac{m}{d}$ . In contrast, without any extra assumptions, our results in Theorem 2 for PRIVIX and HEAPRFX are respectively  $RB = O\left(\frac{(d+m)}{\epsilon} \log\left(\frac{d^2}{m\epsilon\delta} + d\right)\right)$  and  $RB = O\left(\frac{d}{\epsilon} \log\left(\frac{d^2}{m\epsilon\delta}\right)\right)$  which improves the total communication cost of Theorem 1 in [37] under regimes such that  $\frac{1}{\epsilon} \geq d$  or  $d \gg m$ . Theorem 2 in [37] is based the *Sliding Window Heavy Hitters* assumption, which is similar to the gradient diversity assumption in [29, 12]. Under that assumption the total communication cost is shown to be  $RB = O\left(\frac{m \max(I^{2/3}, 2 - \alpha)}{\epsilon^3 \alpha} \log\left(\frac{d \max(I^{2/3}, 2 - \alpha)}{\epsilon^3 \delta}\right)\right)$  where  $I$  is a constant related to the window of gradients. We improve this bound under weaker assumptions in a regime where  $\frac{I^{2/3}}{\epsilon^2} \geq d$ . We also provide bounds for PL, convex and non-convex objectives contrary to [37]. Finally, we note that algorithms in [37] are using momentum at server. While we do not use it explicitly, we can modify our algorithms to include momentum easily.

## 5 Numerical Study

In this section, we provide empirical results on MNIST benchmark dataset to demonstrate the effectiveness of our proposed algorithms. We train LeNet-5 Convolutional Neural Network (CNN) architecture introduced in [24], with 60 000 parameters. We compare Federated SGD (FedSGD) as the full-precision baseline, along with four sketching methods SketchSGD [17], FetchSGD [37], and two FedSketch variants FS-PRIVIX and FS-HEAPRFX. Note that in Algorithm 3, FS-PRIVIX with global learning rate  $\gamma = 1$  is equivalent to the DiffSketch algorithm proposed in [29]. Also, SketchSGD is slightly modified to compress the change in local weights (instead of local gradient in every iteration), and FetchSGD is implemented with second round of communication for fairness. (The original proposal does not include second round of communication, which performs worse with small sketch size.) As suggested in [37], the momentum factor of FetchSGD is set to 0.9, and we also follow some recommended implementation tricks to improve its performance, which are detailed in the Appendix. The number of workers is set to 50 and we report the results for 1 and 5 local epochs.



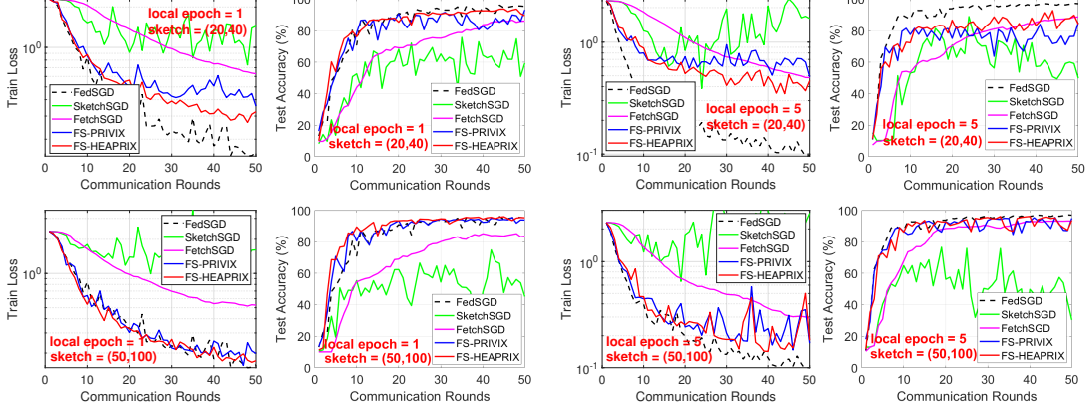


Figure 2: Heterogeneous case: Comparison of compressed optimization algorithms on LeNet CNN.

A local epoch is finished when all workers go through their local data samples once. The local batch size is 30. In each round, we randomly choose half of the devices to be active. We tune the learning rates ( $\eta$  and  $\gamma$ , if applicable) over log-scale and report the best results, for both *homogeneous* and *heterogeneous* setting. In the former case, each device receives uniformly drawn data samples, and in the latter, it only receives samples from one or two classes among ten.

**Homogeneous case.** In Figure 1, we provide the training loss and test accuracy with different number of local epochs and sketch size,  $(t, k) = (20, 40)$  and  $(50, 100)$ . Note that, these two choices of sketch size correspond to a  $75\times$  and  $12\times$  compression ratio, respectively. We conclude

- In general, increasing compression ratio would sacrifice learning performance. In all cases, FS-HEAPRIX performs the best in terms of both training objective and test accuracy, among all compressed methods.
- FS-HEAPRIX is better than FS-PRIVIX, especially with small sketches (high compression ratio). FS-HEAPRIX yields acceptable extra test error compared to full-precision FedSGD, particularly when considering the high compression ratio (e.g.,  $75\times$ ).
- From the training loss, we see that the performance of FS-HEAPRIX improves when the number of local updates increases. *That is, the proposed method is able to further reduce the communication cost by reducing the number of rounds required for communication.* This is also consistent with our theoretical findings.

In general, our proposed FS-HEAPRIX outperforms all competing methods, and a sketch size of  $(50, 100)$  is sufficient to approach the accuracy of full-precision FedSGD.

**Heterogeneous case.** We plot similar set of results in Figure 2 for non-i.i.d. data distribution, which leads to more twists and turns in the training curves. We see that SketchSGD performs very poorly in the heterogeneous case, which is improved by error tracking and momentum in FetchSGD, as expected. However, both of these methods are worse than our proposed FedSketchGATE methods, which can achieve similar generalization accuracy as full-precision FedSGD, even with small sketch size (i.e.,  $75\times$  compression with 1 local epoch). Note that, slower convergence and worse generalization of FedSGD in non-i.i.d. data distribution case is also reported in e.g. [33, 8].

We also notice in Figure 2 the advantage of FS-HEAPRIX over FS-PRIVIX in terms of training loss and test accuracy. However, empirically we see that in the heterogeneous setting, more local updates tend to undermine the learning performance, especially with small sketch size. Nevertheless, when the sketch size is not too small, i.e.,  $(50, 100)$ , FS-HEAPRIX can still provide comparable test accuracy as FedSGD in both cases. Our empirical study demonstrates that our proposed FedSketch (and FedSketchGATE) frameworks are able to perform well in homogeneous (resp. heterogeneous) setting, with high compression rate. In particular, FedSketch methods are advantageous over recent SketchSGD [17] and FetchSGD [37] in all cases. FS-HEAPRIX performs the best among all the tested compressed optimization algorithms, which in many cases achieves similar generalization accuracy as full-precision FedSGD with small sketch size.

## 6 Conclusion

In this paper, we introduced FedSKETCH and FedSKETCHGATE algorithms for homogeneous and heterogeneous data distribution setting respectively for Federated Learning wherein communication between server and devices is only performed using count sketch. Our algorithms, thus, provide communication-efficiency and privacy, through random hashes based sketches. We analyze the convergence error for *non-convex*, *PL* and *general convex* objective functions in the scope of Federated Optimization. We provide insightful numerical experiments showcasing the advantages of our FedSKETCH and FedSKETCHGATE methods over current federated optimization algorithm. The proposed algorithms outperform competing compression method and can achieve comparable test accuracy as Federated SGD, with high compression ratio.

## References

- [1] D. Alistarh, D. Grubic, J. Li, R. Tomioka, and M. Vojnovic. Qsgd: Communication-efficient sgd via gradient quantization and encoding. In *Advances in Neural Information Processing Systems (NIPS)*, pages 1709–1720, Long Beach, 2017.
- [2] D. Alistarh, T. Hoefler, M. Johansson, N. Konstantinov, S. Khirirat, and C. Renggli. The convergence of sparsified gradient methods. In *Advances in Neural Information Processing Systems (NeurIPS)*, pages 5973–5983, Montréal, Canada, 2018.
- [3] D. Basu, D. Data, C. Karakus, and S. N. Diggavi. Qsparse-local-sgd: Distributed SGD with quantization, sparsification and local computations. In *Advances in Neural Information Processing Systems (NeurIPS)*, pages 14668–14679, Vancouver, Canada, 2019.
- [4] J. Bernstein, Y. Wang, K. Azizzadenesheli, and A. Anandkumar. SIGNSGD: compressed optimisation for non-convex problems. In *Proceedings of the 35th International Conference on Machine Learning (ICML)*, pages 559–568, Stockholmsmässan, Stockholm, Sweden, 2018.
- [5] K. Bonawitz, V. Ivanov, B. Kreuter, A. Marcedone, H. B. McMahan, S. Patel, D. Ramage, A. Segal, and K. Seth. Practical secure aggregation for privacy-preserving machine learning. In *Proceedings of the 2017 ACM SIGSAC Conference on Computer and Communications Security (CCS)*, pages 1175–1191, Dallas, TX, 2017.
- [6] L. Bottou and O. Bousquet. The tradeoffs of large scale learning. In *Advances in Neural Information Processing Systems (NIPS)*, pages 161–168, Vancouver, Canada, 2008.
- [7] M. Charikar, K. C. Chen, and M. Farach-Colton. Finding frequent items in data streams. *Theoretical Computer Science*, 312(1):3–15, 2004. doi: 10.1016/S0304-3975(03)00400-6. URL [https://doi.org/10.1016/S0304-3975\(03\)00400-6](https://doi.org/10.1016/S0304-3975(03)00400-6).
- [8] X. Chen, X. Li, and P. Li. Toward communication efficient adaptive gradient method. In *ACM-IMS Foundations of Data Science Conference (FODS)*, Seattle, WA, 2020.
- [9] G. Cormode and S. Muthukrishnan. An improved data stream summary: the count-min sketch and its applications. *Journal of Algorithms*, 55(1):58–75, 2005.
- [10] C. Dwork. Differential privacy. In *Automata, Languages and Programming, 33rd International Colloquium, ICALP 2006, Venice, Italy, July 10-14, 2006, Proceedings, Part II*, volume 4052 of *Lecture Notes in Computer Science*, pages 1–12. Springer, 2006.
- [11] R. C. Geyer, T. Klein, and M. Nabi. Differentially private federated learning: A client level perspective. *arXiv preprint arXiv:1712.07557*, 2017.
- [12] F. Haddadpour and M. Mahdavi. On the convergence of local descent methods in federated learning. *arXiv preprint arXiv:1910.14425*, 2019.
- [13] F. Haddadpour, M. M. Kamani, A. Mokhtari, and M. Mahdavi. Federated learning with compression: Unified analysis and sharp guarantees. *arXiv preprint arXiv:2007.01154*, 2020.
- [14] S. Hardy, W. Henecka, H. Ivey-Law, R. Nock, G. Patrini, G. Smith, and B. Thorne. Private federated learning on vertically partitioned data via entity resolution and additively homomorphic encryption. *arXiv preprint arXiv:1711.10677*, 2017.
- [15] S. Horváth and P. Richtárik. A better alternative to error feedback for communication-efficient distributed learning. *arXiv preprint arXiv:2006.11077*, 2020.
- [16] S. Horváth, D. Kovalev, K. Mishchenko, S. Stich, and P. Richtárik. Stochastic distributed learning with gradient quantization and variance reduction. *arXiv preprint arXiv:1904.05115*, 2019.
- [17] N. Ivkin, D. Rothchild, E. Ullah, V. Braverman, I. Stoica, and R. Arora. Communication-efficient distributed SGD with sketching. In *Advances in Neural Information Processing Systems (NeurIPS)*, pages 13144–13154, Vancouver, Canada, 2019.
- [18] P. Kairouz, H. B. McMahan, B. Avent, A. Bellet, M. Bennis, A. N. Bhagoji, K. Bonawitz, Z. Charles, G. Cormode, R. Cummings, et al. Advances and open problems in federated learning. *arXiv preprint arXiv:1912.04977*, 2019.
- [19] H. Karimi, J. Nutini, and M. Schmidt. Linear convergence of gradient and proximal-gradient methods under the polyak-łojasiewicz condition. In *Proceedings of European Conference on Machine Learning and Knowledge Discovery in Databases (ECML-PKDD)*, pages 795–811, Riva del Garda, Italy, 2016.

- [20] S. P. Karimireddy, S. Kale, M. Mohri, S. J. Reddi, S. U. Stich, and A. T. Suresh. Scaffold: Stochastic controlled averaging for on-device federated learning. *arXiv preprint arXiv:1910.06378*, 2019.
- [21] A. Khaled, K. Mishchenko, and P. Richtárik. Tighter theory for local SGD on identical and heterogeneous data. In *The 23rd International Conference on Artificial Intelligence and Statistics (AISTATS)*, pages 4519–4529, Online [Palermo, Sicily, Italy], 2020.
- [22] J. Kleinberg. Bursty and hierarchical structure in streams. *Data Mining and Knowledge Discovery*, 7(4):373–397, 2003.
- [23] J. Konečný, H. B. McMahan, F. X. Yu, P. Richtárik, A. T. Suresh, and D. Bacon. Federated learning: Strategies for improving communication efficiency. *arXiv preprint arXiv:1610.05492*, 2016.
- [24] Y. LeCun, L. Bottou, Y. Bengio, and P. Haffner. Gradient-based learning applied to document recognition. *Proceedings of the IEEE*, 86(11):2278–2324, 1998.
- [25] P. Li, K. W. Church, and T. Hastie. One sketch for all: Theory and application of conditional random sampling. In *Advances in Neural Information Processing Systems (NIPS)*, pages 953–960, Vancouver, Canada, 2008.
- [26] T. Li, Z. Liu, V. Sekar, and V. Smith. Privacy for free: Communication-efficient learning with differential privacy using sketches. *arXiv preprint arXiv:1911.00972*, 2019.
- [27] T. Li, A. K. Sahu, A. Talwalkar, and V. Smith. Federated learning: Challenges, methods, and future directions. *IEEE Signal Process. Mag.*, 37(3):50–60, 2020.
- [28] T. Li, A. K. Sahu, A. Talwalkar, and V. Smith. Federated learning: Challenges, methods, and future directions. *IEEE Signal Processing Magazine*, 37(3):50–60, 2020.
- [29] T. Li, A. K. Sahu, M. Zaheer, M. Sanjabi, A. Talwalkar, and V. Smith. Federated optimization in heterogeneous networks. In *Proceedings of Machine Learning and Systems (MLSys)*, Austin, TX, 2020.
- [30] X. Li, K. Huang, W. Yang, S. Wang, and Z. Zhang. On the convergence of fedavg on non-iid data. In *Proceedings of the 8th International Conference on Learning Representations (ICLR)*, Addis Ababa, Ethiopia, 2020.
- [31] X. Liang, S. Shen, J. Liu, Z. Pan, E. Chen, and Y. Cheng. Variance reduced local sgd with lower communication complexity. *arXiv preprint arXiv:1912.12844*, 2019.
- [32] Y. Lin, S. Han, H. Mao, Y. Wang, and B. Dally. Deep gradient compression: Reducing the communication bandwidth for distributed training. In *Proceedings of the 6th International Conference on Learning Representations (ICLR)*, Vancouver, Canada, 2018.
- [33] B. McMahan, E. Moore, D. Ramage, S. Hampson, and B. A. y Arcas. Communication-efficient learning of deep networks from decentralized data. In *Proceedings of the 20th International Conference on Artificial Intelligence and Statistics (AISTATS)*, pages 1273–1282, Fort Lauderdale, FL, 2017.
- [34] H. B. McMahan, D. Ramage, K. Talwar, and L. Zhang. Learning differentially private recurrent language models. In *Proceedings of the 6th International Conference on Learning Representations (ICLR)*, Vancouver, Canada, 2018.
- [35] C. Philippenko and A. Dieuleveut. Artemis: tight convergence guarantees for bidirectional compression in federated learning. *arXiv preprint arXiv:2006.14591*, 2020.
- [36] A. Reisizadeh, A. Mokhtari, H. Hassani, A. Jadbabaie, and R. Pedarsani. Fedpaq: A communication-efficient federated learning method with periodic averaging and quantization. In *The 23rd International Conference on Artificial Intelligence and Statistics (AISTATS)*, pages 2021–2031, Online [Palermo, Sicily, Italy], 2020.
- [37] D. Rothchild, A. Panda, E. Ullah, N. Ivkin, I. Stoica, V. Braverman, J. Gonzalez, and R. Arora. FetchSGD: Communication-efficient federated learning with sketching. *arXiv preprint arXiv:2007.07682*, 2020.
- [38] A. K. Sahu, T. Li, M. Sanjabi, M. Zaheer, A. Talwalkar, and V. Smith. On the convergence of federated optimization in heterogeneous networks. *arXiv preprint arXiv:1812.06127*, 2018.
- [41] S. U. Stich. Local sgd converges fast and communicates little. In *Proceedings of the 7th International Conference on Learning Representations (ICLR)*, New Orleans, LA, 2019.

- 499 [39] S. U. Stich and S. P. Karimireddy. The error-feedback framework: Better rates for sgd with  
500 delayed gradients and compressed communication. *arXiv preprint arXiv:1909.05350*, 2019.
- 501 [40] S. U. Stich, J.-B. Cordonnier, and M. Jaggi. Sparsified sgd with memory. In *Advances in Neural*  
502 *Information Processing Systems (NeurIPS)*, pages 4447–4458, Montréal, Canada, 2018.
- 503 [42] H. Tang, S. Gan, C. Zhang, T. Zhang, and J. Liu. Communication compression for decentralized  
504 training. In *Advances in Neural Information Processing Systems (NeurIPS)*, pages 7652–7662,  
505 Montréal, Canada, 2018.
- 506 [43] J. Wang and G. Joshi. Cooperative sgd: A unified framework for the design and analysis of  
507 communication-efficient sgd algorithms. *arXiv preprint arXiv:1808.07576*, 2018.
- 508 [44] W. Wen, C. Xu, F. Yan, C. Wu, Y. Wang, Y. Chen, and H. Li. Terngrad: Ternary gradients  
509 to reduce communication in distributed deep learning. In *Advances in neural information*  
510 *processing systems (NIPS)*, pages 1509–1519, Long Beach, CA, 2017.
- 511 [45] J. Wu, W. Huang, J. Huang, and T. Zhang. Error compensated quantized sgd and its applications  
512 to large-scale distributed optimization. *arXiv preprint arXiv:1806.08054*, 2018.
- 513 [46] H. Yu, R. Jin, and S. Yang. On the linear speedup analysis of communication efficient momen-  
514 tum SGD for distributed non-convex optimization. In *Proceedings of the 36th International*  
515 *Conference on Machine Learning (ICML)*, pages 7184–7193, Long Beach, CA, 2019.
- 516 [47] H. Yu, S. Yang, and S. Zhu. Parallel restarted SGD with faster convergence and less communi-  
517 cation: Demystifying why model averaging works for deep learning. In *The Thirty-Third AAAI*  
518 *Conference on Artificial Intelligence (AAAI)*, pages 5693–5700, Honolulu, HI, 2019.
- 519 [48] F. Zhou and G. Cong. On the convergence properties of a k-step averaging stochastic gradient  
520 descent algorithm for nonconvex optimization. In *Proceedings of the Twenty-Seventh Inter-*  
521 *national Joint Conference on Artificial Intelligence (IJCAI)*, pages 3219–3227, Stockholm,  
522 Sweden, 2018.

## Checklist

### 1. For all authors...

- (a) Do the main claims made in the abstract and introduction accurately reflect the paper's contributions and scope? **[TODO]**
- (b) Did you describe the limitations of your work? **[TODO]**
- (c) Did you discuss any potential negative societal impacts of your work? **[TODO]**
- (d) Have you read the ethics review guidelines and ensured that your paper conforms to them? **[TODO]**

### 2. If you are including theoretical results...

- (a) Did you state the full set of assumptions of all theoretical results? **[TODO]**
- (b) Did you include complete proofs of all theoretical results? **[TODO]**

### 3. If you ran experiments...

- (a) Did you include the code, data, and instructions needed to reproduce the main experimental results (either in the supplemental material or as a URL)? **[TODO]**
- (b) Did you specify all the training details (e.g., data splits, hyperparameters, how they were chosen)? **[TODO]**
- (c) Did you report error bars (e.g., with respect to the random seed after running experiments multiple times)? **[TODO]**
- (d) Did you include the total amount of compute and the type of resources used (e.g., type of GPUs, internal cluster, or cloud provider)? **[TODO]**

### 4. If you are using existing assets (e.g., code, data, models) or curating/releasing new assets...

- (a) If your work uses existing assets, did you cite the creators? **[TODO]**
- (b) Did you mention the license of the assets? **[TODO]**
- (c) Did you include any new assets either in the supplemental material or as a URL? **[TODO]**
- (d) Did you discuss whether and how consent was obtained from people whose data you're using/curating? **[TODO]**
- (e) Did you discuss whether the data you are using/curating contains personally identifiable information or offensive content? **[TODO]**

### 5. If you used crowdsourcing or conducted research with human subjects...

- (a) Did you include the full text of instructions given to participants and screenshots, if applicable? **[TODO]**
- (b) Did you describe any potential participant risks, with links to Institutional Review Board (IRB) approvals, if applicable? **[TODO]**
- (c) Did you include the estimated hourly wage paid to participants and the total amount spent on participant compensation? **[TODO]**

## 559 A Notations and Definitions

560 **Notation.** Here we denote the count sketch of the vector  $\mathbf{x}$  by  $\mathbf{S}(\mathbf{x})$  and with an abuse of notation,  
 561 we indicate the expectation over the randomness of count sketch with  $\mathbb{E}_{\mathbf{S}}[\cdot]$ . We illustrate the random  
 562 subset of the devices selected by the central server with  $\mathcal{K}$  with size  $|\mathcal{K}| = k \leq p$ , and we represent  
 563 the expectation over the device sampling with  $\mathbb{E}_{\mathcal{K}}[\cdot]$ .

Table 1: Table of Notations

$p$	$\triangleq$	Number of devices
$k$	$\triangleq$	Number of sampled devices for homogeneous setting
$\mathcal{K}^{(r)}$	$\triangleq$	Set of sampled devices in communication round $r$
$d$	$\triangleq$	Dimension of the model
$\tau$	$\triangleq$	Number of local updates
$R$	$\triangleq$	Number of communication rounds
$B$	$\triangleq$	Size of transmitted bits
$R \times B$	$\triangleq$	Total communication cost per device
$\kappa$	$\triangleq$	Condition number
$\epsilon$	$\triangleq$	Target accuracy
$\mu$	$\triangleq$	PL constant
$m$	$\triangleq$	Number of bins of hash tables
$\mathbf{S}(\mathbf{x})$	$\triangleq$	Count sketch of the vector $\mathbf{x}$
$\mathbb{U}(\Delta)$	$\triangleq$	Class of unbiased compressor, see Definition 1

564 **Definition 3** (Polyak-Łojasiewicz). *A function  $f(\mathbf{x})$  satisfies the Polyak-Łojasiewicz(PL) condition*  
 565 *with constant  $\mu$  if  $\frac{1}{2}\|\nabla f(\mathbf{x})\|_2^2 \geq \mu(f(\mathbf{x}) - f(\mathbf{x}^*))$ ,  $\forall \mathbf{x} \in \mathbb{R}^d$  with  $\mathbf{x}^*$  is an optimal solution.*

### 566 A.1 Count sketch

567 In this paper, we exploit the commonly used Count Sketch [7] which is described in Algorithm 5.

---

#### Algorithm 5 Count Sketch (CS) [7]

---

```

1: Inputs:  $\mathbf{x} \in \mathbb{R}^d, t, k, \mathbf{S}_{m \times t}, h_j(1 \leq i \leq t), \text{sign}_j(1 \leq i \leq t)$ 
2: Compress vector  $\mathbf{x} \in \mathbb{R}^d$  into  $\mathbf{S}(\mathbf{x})$ :
3: for  $x_i \in \mathbf{x}$  do
4:   for  $j = 1, \dots, t$  do
5:      $\mathbf{S}[j][h_j(i)] = \mathbf{S}[j-1][h_{j-1}(i)] + \text{sign}_j(i) \cdot x_i$ 
6:   end for
7: end for
8: return  $\mathbf{S}_{m \times t}(\mathbf{x})$ 

```

---

### 568 A.2 PRIVIX and compression error of HEAPRIX

569 For the sake of completeness we review PRIVIX algorithm that is also mentioned in [26] as follows:

---

#### Algorithm 6 PRIVIX/DiffSketch [26]: Unbiased compressor based on sketching.

---

```

1: Inputs:  $\mathbf{x} \in \mathbb{R}^d, t, m, \mathbf{S}_{m \times t}, h_j(1 \leq i \leq t), \text{sign}_j(1 \leq i \leq t)$ 
2: Query  $\tilde{\mathbf{x}} \in \mathbb{R}^d$  from  $\mathbf{S}(\mathbf{x})$ :
3: for  $i = 1, \dots, d$  do
4:    $\tilde{\mathbf{x}}[i] = \text{Median}\{\text{sign}_j(i) \cdot \mathbf{S}[j][h_j(i)] : 1 \leq j \leq t\}$ 
5: end for
6: Output:  $\tilde{\mathbf{x}}$ 

```

---



Table 3: Comparison of results with compression and periodic averaging in the heterogeneous setting. UG and PP stand for Unbounded Gradient and Privacy Property respectively.

Reference	non-convex	General Convex	UG	PP
<b>Basu et al. [3] (with <math>\gamma = m/d</math>)</b>	$R = O\left(\frac{d}{m\epsilon^{1.5}}\right)$ $\tau = O\left(\frac{m}{pd\sqrt{\epsilon}}\right)$ $B = O(d)$ $RB = O\left(\frac{d^2}{m\epsilon^{1.5}}\right)$	—	✗	✗
<b>Li et al. [26]</b>	—	$R = O\left(\frac{d}{m\epsilon^2}\right)$ $\tau = 1$ $B = O\left(m \log\left(\frac{d^2}{m\epsilon^2\delta}\right)\right)$	✗	✓
<b>Rothchild et al. [37]</b>	$R = O\left(\max\left(\frac{1}{\epsilon^2}, \frac{d^2 - md}{m^2\epsilon}\right)\right)$ $\tau = 1$ $B = O\left(m \log\left(\frac{d}{\delta} \max\left(\frac{1}{\epsilon^2}, \frac{d^2 - md}{m^2\epsilon}\right)\right)\right)$ $RB = O\left(m \max\left(\frac{1}{\epsilon^2}, \frac{d^2 - md}{m^2\epsilon}\right) \log\left(\frac{d}{\delta} \max\left(\frac{1}{\epsilon^2}, \frac{d^2 - md}{m^2\epsilon}\right)\right)\right)$	—	✗	✗
<b>Rothchild et al. [37]</b>	$R = O\left(\frac{\max(I^{2/3}, 2 - \alpha)}{\epsilon^3}\right)$ $\tau = 1$ $B = O\left(\frac{m}{\alpha} \log\left(\frac{d \max(I^{2/3}, 2 - \alpha)}{\epsilon^3\delta}\right)\right)$ $RB = O\left(\frac{m \max(I^{2/3}, 2 - \alpha)}{\epsilon^3\alpha} \log\left(\frac{d \max(I^{2/3}, 2 - \alpha)}{\epsilon^3\delta}\right)\right)$	—	✗	✗
<b>Theorem 2</b>	$R = O\left(\frac{d}{m\epsilon}\right)$ $\tau = O\left(\frac{1}{p\epsilon}\right)$ $B = O\left(m \log\left(\frac{d^2}{m\epsilon\delta}\right)\right)$ $RB = O\left(\frac{d}{\epsilon} \log\left(\frac{d^2}{m\epsilon\delta} \log\left(\frac{1}{\epsilon}\right)\right)\right)$	$R = O\left(\frac{d}{m\epsilon} \log\left(\frac{1}{\epsilon}\right)\right)$ $\tau = O\left(\frac{1}{p\epsilon^2}\right)$ $B = O\left(m \log\left(\frac{d^2}{m\epsilon\delta}\right)\right)$	✓	✓

Regarding the compression error of sketching we restate the following Corollary from the main body of this paper:

**Corollary 2.** *Based on Theorem 3 of [15] and using Algorithm 2, we have  $C(x) \in \mathbb{U}(c\frac{d}{m})$ . This shows that unlike PRIVIX (Algorithm 6) the compression noise can be made as small as possible using large size of hash table.*

*Proof.* The proof simply follows from Theorem 3 in [15] and Algorithm 2 by setting  $\Delta_1 = c\frac{d}{m}$  and  $\Delta_2 = 1 + c\frac{d}{m}$  we obtain  $\Delta = \Delta_2 + \frac{1 - \Delta_2}{\Delta_1} = c\frac{d}{m} = O\left(\frac{d}{m}\right)$  for the compression error of HEAPR IX.  $\square$

## B Summary of comparison of our results with prior works

For the purpose of further clarification, we summarize the comparison of our results with related works. We recall that  $p$  is the number of devices,  $d$  is the dimension of the model,  $\kappa$  is the condition number,  $\epsilon$  is the target accuracy,  $R$  is the number of communication rounds, and  $\tau$  is the number of local updates. We start with the homogeneous setting comparison. Comparison of our results and existing ones for homogeneous and heterogeneous setting are given respectively Table 2 and Table 3.

Table 2: Comparison of results with compression and periodic averaging in the homogeneous setting. UG and PP stand for Unbounded Gradient and Privacy Property respectively.

Reference	PL/Strongly Convex	UG	PP
<b>Ivkin et al. [17]</b>	$R = O\left(\max\left(\frac{d}{m\sqrt{\epsilon}}, \frac{1}{\epsilon}\right)\right), \tau = 1, B = O\left(m \log\left(\frac{dR}{\delta}\right)\right)$ $pRB = O\left(\frac{pd}{m\epsilon} \log\left(\frac{d}{\delta\sqrt{\epsilon}} \max\left(\frac{d}{m}, \frac{1}{\sqrt{\epsilon}}\right)\right)\right)$	✗	✗
<b>Theorem 1</b>	$R = O\left(\kappa\left(\frac{d-m}{mk} + 1\right) \log\left(\frac{1}{\epsilon}\right)\right), \tau = O\left(\frac{d}{k\left(\frac{d}{k} + m\right)\epsilon}\right), B = O\left(m \log\left(\frac{dR}{\delta}\right)\right)$ $kRB = O\left(m\kappa(d - m + mk) \log\left(\frac{1}{\epsilon}\right) \log\left(\frac{\kappa(d\frac{d-m}{mk} + d) \log\left(\frac{1}{\epsilon}\right)}{\delta}\right)\right)$	✓	✓

**Comparison with [13] and [36]** Convergence analysis of algorithms in [13] relies on unbiased compression, while in this paper our FL algorithm based on HEAPRIX enjoys from unbiased compression with equivalent biased compression variance. Moreover, we highlight that the convergence analysis of FedCOMGATE is based on the extra assumption of boundedness of the difference between the average of compressed vectors and compressed averages of vectors. However, we do not need this extra assumption as it is satisfied naturally due to linearity of sketching. Finally, as pointed out in Remark 2, our algorithms enjoy from a bidirectional compression property, unlike FedCOMGATE in general. Furthermore, since results in [13] improve the communication complexity of FedPAQ algorithm, developed in [36], hence FedSKETCH and FedSKETCHGATE improves the communication complexity obtained in [36].

**Comparison with [3].** We note that the algorithm in [3] uses a composed compression and quantization while our algorithm is solely based on compression. So, in order to compare with algorithms in [3] we only consider Qsparse-local-SGD with compression and we let compression factor  $\gamma = \frac{m}{d}$  (to compare with the same compression ratio induced with sketch size of  $mt$ ). For strongly convex objective in Qsparse-local-SGD to achieve convergence error of  $\epsilon$  they require  $R = O\left(\kappa \frac{d}{m\sqrt{\epsilon}}\right)$  and  $\tau = O\left(\frac{m}{pd\sqrt{\epsilon}}\right)$ , which is improved to  $R = O\left(\frac{\kappa d}{m} \log(1/\epsilon)\right)$  and  $\tau = O\left(\frac{1}{p\epsilon}\right)$  for PL objectives. Similarly, for non-convex objective [3] requires  $R = O\left(\frac{d}{m\epsilon^{1.5}}\right)$  and  $\tau = O\left(\frac{m}{pd\sqrt{\epsilon}}\right)$ , which is improved to  $R = O\left(\frac{d}{m\epsilon}\right)$  and  $\tau = O\left(\frac{1}{p\epsilon}\right)$ . We note that we reduce communication rounds at the cost of increasing number of local updates (which scales down with number of devices,  $p$ ). Additionally, we highlight that our FedSKETCHGATE exploits the gradient tracking idea to deal with data heterogeneity, while algorithms in [3] does not develop such mechanism and may suffer from poor convergence in heterogeneous setting. We also note that setting  $\tau = 1$  and using  $top_m$  compressor, the QSPARSE-local-SGD algorithm becomes similar to distributed SGD with sketching as they both use the error feedback framework to improve the compression variance. Finally, since the average of sparse vectors may not be sparse in general the number of transmitted bits from server to devices in QSPARSE-Local-SGD in [3] may not be sparse in general ( $B = O(d)$ ), however our algorithms enjoy from bidirectional compression properly due to lower dimension and linearity properties of sketching ( $B = O(m \log(\frac{Rd}{\delta}))$ ). Therefore, the total number of bits per device for strongly convex and non-convex objective is improved respectively from  $RB = O\left(\kappa \frac{d^2}{m\sqrt{\epsilon}}\right)$  and  $RB = O\left(\frac{d^2}{m\epsilon^{1.5}}\right)$  in [3] to  $RB = O\left(\kappa d \log(\frac{\kappa d^2}{m\delta} \log(1/\epsilon)) \log(1/\epsilon)\right) = O\left(\kappa d \max\left(\log(\frac{\kappa d^2}{m\delta}), \log^2(1/\epsilon)\right)\right)$  and  $RB = O\left(\log(\frac{d^2}{m\epsilon\delta}) \frac{d}{\epsilon}\right)$ .

Additionally, as we noted using sketching for transmission implies two way communication from master to devices and vice versa. Therefore, in order to show efficacy of our algorithm we compare our convergence analysis with the obtained rates in the following related work:

**Comparison with [35].** The reference [35] considers two-way compression from parameter server to devices and vice versa. They provide the convergence rate of  $R = O\left(\frac{\omega^{\text{Up}} \omega^{\text{Down}}}{\epsilon^2}\right)$  for strongly-objective functions where  $\omega^{\text{Up}}$  and  $\omega^{\text{Down}}$  are uplink and downlink's compression noise (specializing to our case for the sake of comparison  $\omega^{\text{Up}} = \omega^{\text{Down}} = \theta(d)$ ) for general heterogeneous data distribution. In contrast, while our algorithms are using bidirectional compression due to use of sketching for communication, our convergence rate for strongly-convex objective is  $R = O(\kappa \mu^2 d \log(\frac{1}{\epsilon}))$  with probability  $1 - \delta$ .

We would like to also mention that there prior studies such as [?] and [?] that analyze the two-way compression, but since [35] is the state-of-the-art on this topic we only compared our results with these papers.

## C Theoretical Proofs

We will use the following fact (which is also used in [30, 12]) in proving results.

**Fact 3** ([30, 12]). Let  $\{x_i\}_{i=1}^p$  denote any fixed deterministic sequence. We sample a multiset  $\mathcal{P}$  (with size  $K$ ) uniformly at random where  $x_j$  is sampled with probability  $q_j$  for  $1 \leq j \leq p$  with replacement.

632 Let  $\mathcal{P} = \{i_1, \dots, i_K\} \subset [p]$  (some  $i_j$ s may have the same value). Then

$$\mathbb{E}_{\mathcal{P}} \left[ \sum_{i \in \mathcal{P}} x_i \right] = \mathbb{E}_{\mathcal{P}} \left[ \sum_{k=1}^K x_{i_k} \right] = K \mathbb{E}_{\mathcal{P}} [x_{i_k}] = K \left[ \sum_{j=1}^p q_j x_j \right] \quad (2)$$

633 For the sake of the simplicity, we review an assumption for the quantization/compression, that  
 634 naturally holds for PRIVIX and HEAPRIX.

635 **Assumption 4** ([13]). *The output of the compression operator  $Q(\mathbf{x})$  is an unbiased estimator of*  
 636 *its input  $\mathbf{x}$ , and its variance grows with the squared of the squared of  $\ell_2$ -norm of its argument, i.e.,*  
 637  $\mathbb{E}[Q(\mathbf{x})] = \mathbf{x}$  *and*  $\mathbb{E}[\|Q(\mathbf{x}) - \mathbf{x}\|^2] \leq \omega \|\mathbf{x}\|^2$ .

638 We note that the sketching PRIVIX and HEAPRIX, satisfy Assumption 4 with  $\omega = c \frac{d}{m}$  and  $\omega =$   
 639  $c \frac{d}{m} - 1$  respectively with probability  $1 - \frac{\delta}{R}$  per communication round. Therefore, all the results in  
 640 Theorem 1, by taking union over the all probabilities of each communication rounds, are concluded  
 641 with probability  $1 - \delta$  by plugging  $\omega = c \frac{d}{m}$  and  $\omega = c \frac{d}{m} - 1$  respectively into the corresponding  
 642 convergence bounds.

### 643 C.1 Proof of Theorem 1

644 In this section, we study the convergence properties of our FedSKETCH method presented in Algo-  
 645 rithm 3. Before developing the proofs for FedSKETCH in the homogeneous setting, we first mention  
 646 the following intermediate lemmas.

647 **Lemma 1.** *Using unbiased compression and under Assumption 2, we have the following bound:*

$$\mathbb{E}_{\mathcal{K}} \left[ \mathbb{E}_{\mathbf{S}, \xi^{(r)}} [\|\tilde{\mathbf{g}}_{\mathbf{S}}^{(r)}\|^2] \right] = \mathbb{E}_{\xi^{(r)}} \mathbb{E}_{\mathbf{S}} [\|\tilde{\mathbf{g}}_{\mathbf{S}}^{(r)}\|^2] \leq \tau \left( \frac{\omega}{k} + 1 \right) \sum_{j=1}^m q_j \left[ \sum_{c=0}^{\tau-1} \|\mathbf{g}_j^{(c,r)}\|^2 + \sigma^2 \right] \quad (3)$$

*Proof.*

$$\begin{aligned} & \mathbb{E}_{\xi^{(r)} | \mathbf{w}^{(r)}} \mathbb{E}_{\mathcal{K}} \left[ \mathbb{E}_{\mathbf{S}} \left[ \left\| \frac{1}{k} \sum_{j \in \mathcal{K}} \mathbf{S} \left( \sum_{c=0}^{\tau-1} \tilde{\mathbf{g}}_j^{(c,r)} \right) \right\|^2 \right] \right] \\ &= \mathbb{E}_{\xi^{(r)}} \left[ \mathbb{E}_{\mathcal{K}} \left[ \mathbb{E}_{\mathbf{S}} \left[ \left\| \frac{1}{k} \sum_{j \in \mathcal{K}} \mathbf{S} \underbrace{\left( \sum_{c=0}^{\tau-1} \tilde{\mathbf{g}}_j^{(c,r)} \right)}_{\tilde{\mathbf{g}}_{\mathbf{S}_j}^{(r)}} \right\|^2 \right] \right] \right] \\ &\stackrel{\textcircled{1}}{=} \mathbb{E}_{\xi^{(r)}} \left[ \mathbb{E}_{\mathcal{K}} \left[ \left\| \frac{1}{k} \sum_{j \in \mathcal{K}} \tilde{\mathbf{g}}_{\mathbf{S}_j}^{(r)} - \frac{1}{k} \sum_{j \in \mathcal{K}} \mathbb{E}_{\mathbf{S}} [\tilde{\mathbf{g}}_{\mathbf{S}_j}^{(r)}] \right\|^2 + \left\| \mathbb{E}_{\mathbf{S}} \left[ \frac{1}{k} \sum_{j \in \mathcal{K}} \tilde{\mathbf{g}}_{\mathbf{S}_j}^{(r)} \right] \right\|^2 \right] \right] \\ &\stackrel{\textcircled{2}}{=} \mathbb{E}_{\xi^{(r)}} \left[ \mathbb{E}_{\mathcal{K}} \left[ \mathbb{E}_{\mathbf{S}} \left[ \left\| \frac{1}{k} \left[ \sum_{j \in \mathcal{K}} \tilde{\mathbf{g}}_{\mathbf{S}_j}^{(r)} - \sum_{j \in \mathcal{K}} \tilde{\mathbf{g}}_j^{(r)} \right] \right\|^2 + \left\| \frac{1}{k} \sum_{j \in \mathcal{K}} \tilde{\mathbf{g}}_j^{(r)} \right\|^2 \right] \right] \right] \\ &= \mathbb{E}_{\xi^{(r)}} \left[ \mathbb{E}_{\mathcal{K}} \left[ \left[ \text{Var}_{\mathbf{S}} \left[ \frac{1}{k} \sum_{j \in \mathcal{K}} \tilde{\mathbf{g}}_{\mathbf{S}_j}^{(r)} \right] + \left\| \frac{1}{k} \sum_{j \in \mathcal{K}} \tilde{\mathbf{g}}_j^{(r)} \right\|^2 \right] \right] \right] \\ &= \mathbb{E}_{\xi^{(r)}} \left[ \mathbb{E}_{\mathcal{K}} \left[ \left[ \frac{1}{k^2} \sum_{j \in \mathcal{K}} \text{Var}_{\mathbf{S}_j} [\tilde{\mathbf{g}}_{\mathbf{S}_j}^{(r)}] + \left\| \frac{1}{k} \sum_{j \in \mathcal{K}} \tilde{\mathbf{g}}_j^{(r)} \right\|^2 \right] \right] \right] \end{aligned}$$

$$\begin{aligned}
&\leq \mathbb{E}_{\xi^{(r)}} \left[ \mathbb{E}_{\mathcal{K}} \left[ \frac{1}{k^2} \sum_{j \in \mathcal{K}} \omega \left\| \tilde{\mathbf{g}}_j^{(r)} \right\|^2 + \left\| \frac{1}{k} \sum_{j \in \mathcal{K}} \tilde{\mathbf{g}}_j^{(r)} \right\|^2 \right] \right] \\
&= \left[ \mathbb{E}_{\xi} \left[ \frac{1}{k} \sum_{j \in \mathcal{K}} \omega \left\| \tilde{\mathbf{g}}_j^{(r)} \right\|^2 + \mathbb{E}_{\mathcal{K}} \mathbb{E}_{\xi^{(r)}} \left\| \frac{1}{k} \sum_{j \in \mathcal{K}} \tilde{\mathbf{g}}_j^{(r)} \right\|^2 \right] \right] \\
&= \left[ \mathbb{E}_{\xi} \left[ \frac{\omega}{k} \sum_{j=1}^p q_j \left\| \tilde{\mathbf{g}}_j^{(r)} \right\|^2 + \mathbb{E}_{\mathcal{K}} \left[ \text{Var} \left( \frac{1}{k} \sum_{j \in \mathcal{K}} \tilde{\mathbf{g}}_j^{(r)} \right) + \left\| \frac{1}{k} \sum_{j \in \mathcal{K}} \mathbf{g}_j^{(r)} \right\|^2 \right] \right] \right] \\
&= \frac{\omega}{k} \sum_{j=1}^p q_j \mathbb{E}_{\xi} \left\| \tilde{\mathbf{g}}_j^{(r)} \right\|^2 + \mathbb{E}_{\mathcal{K}} \left[ \frac{1}{k^2} \sum_{j \in \mathcal{K}} \text{Var} \left( \tilde{\mathbf{g}}_j^{(r)} \right) + \left\| \frac{1}{k} \sum_{j \in \mathcal{K}} \mathbf{g}_j^{(r)} \right\|^2 \right] \\
&\leq \frac{\omega}{k} \sum_{j=1}^p q_j \mathbb{E}_{\xi} \left\| \tilde{\mathbf{g}}_j^{(r)} \right\|^2 + \mathbb{E}_{\mathcal{K}} \left[ \frac{1}{k^2} \sum_{j \in \mathcal{K}} \tau \sigma^2 + \frac{1}{k} \sum_{j \in \mathcal{K}} \left\| \mathbf{g}_j^{(r)} \right\|^2 \right] \\
&= \frac{\omega}{k} \sum_{j=1}^p q_j \left[ \text{Var} \left( \tilde{\mathbf{g}}_j^{(r)} \right) + \left\| \mathbf{g}_j^{(r)} \right\|^2 \right] + \left[ \frac{\tau \sigma^2}{k} + \sum_{j=1}^p q_j \left\| \mathbf{g}_j^{(r)} \right\|^2 \right] \\
&\leq \frac{\omega}{k} \sum_{j=1}^p q_j \left[ \tau \sigma^2 + \left\| \mathbf{g}_j^{(r)} \right\|^2 \right] + \left[ \frac{\tau \sigma^2}{k} + \sum_{j=1}^p q_j \left\| \mathbf{g}_j^{(r)} \right\|^2 \right] \\
&= (\omega + 1) \frac{\tau \sigma^2}{k} + \left( \frac{\omega}{k} + 1 \right) \left[ \sum_{j=1}^p q_j \left\| \mathbf{g}_j^{(r)} \right\|^2 \right] \tag{4}
\end{aligned}$$

648 where ① holds due to  $\mathbb{E} \left[ \left\| \mathbf{x} \right\|^2 \right] = \text{Var}[\mathbf{x}] + \left\| \mathbb{E}[\mathbf{x}] \right\|^2$ , ② is due to  $\mathbb{E}_{\mathbf{S}} \left[ \frac{1}{p} \sum_{j=1}^p \tilde{\mathbf{g}}_{\mathbf{S}j}^{(r)} \right] = \frac{1}{p} \sum_{j=1}^m \tilde{\mathbf{g}}_j^{(r)}$ .

649 Next we show that from Assumptions 3, we have

$$\mathbb{E}_{\xi^{(r)}} \left[ \left\| \tilde{\mathbf{g}}_j^{(r)} - \mathbf{g}_j^{(r)} \right\|^2 \right] \leq \tau \sigma^2 \tag{5}$$

650 To do so, note that

$$\begin{aligned}
\text{Var} \left( \tilde{\mathbf{g}}_j^{(r)} \right) &= \mathbb{E}_{\xi^{(r)}} \left[ \left\| \tilde{\mathbf{g}}_j^{(r)} - \mathbf{g}_j^{(r)} \right\|^2 \right] \stackrel{\text{①}}{=} \mathbb{E}_{\xi^{(r)}} \left[ \left\| \sum_{c=0}^{\tau-1} \left[ \tilde{\mathbf{g}}_j^{(c,r)} - \mathbf{g}_j^{(c,r)} \right] \right\|^2 \right] = \text{Var} \left( \sum_{c=0}^{\tau-1} \tilde{\mathbf{g}}_j^{(c,r)} \right) \\
&\stackrel{\text{②}}{=} \sum_{c=0}^{\tau-1} \text{Var} \left( \tilde{\mathbf{g}}_j^{(c,r)} \right) \\
&= \sum_{c=0}^{\tau-1} \mathbb{E} \left[ \left\| \tilde{\mathbf{g}}_j^{(c,r)} - \mathbf{g}_j^{(c,r)} \right\|^2 \right] \\
&\stackrel{\text{③}}{\leq} \tau \sigma^2 \tag{6}
\end{aligned}$$

651 where in ① we use the definition of  $\tilde{\mathbf{g}}_j^{(r)}$  and  $\mathbf{g}_j^{(r)}$ , in ② we use the fact that mini-batches are chosen  
652 in i.i.d. manner at each local machine, and ③ immediately follows from Assumptions 2.

653 Replacing  $\mathbb{E}_{\xi^{(r)}} \left[ \left\| \tilde{\mathbf{g}}_j^{(r)} - \mathbf{g}_j^{(r)} \right\|^2 \right]$  in (4) by its upper bound in (5) implies that

$$\mathbb{E}_{\xi^{(r)} | \mathbf{w}^{(r)}} \mathbb{E}_{\mathbf{S}, \mathcal{K}} \left[ \left\| \frac{1}{k} \sum_{j \in \mathcal{K}} \mathbf{S} \left( \sum_{c=0}^{\tau-1} \tilde{\mathbf{g}}_j^{(c,r)} \right) \right\|^2 \right] \leq (\omega + 1) \frac{\tau \sigma^2}{k} + \left( \frac{\omega}{k} + 1 \right) \sum_{j=1}^p q_j \left\| \mathbf{g}_j^{(r)} \right\|^2 \tag{7}$$

654 Further note that we have

$$\left\| \mathbf{g}_j^{(r)} \right\|^2 = \left\| \sum_{c=0}^{\tau-1} \mathbf{g}_j^{(c,r)} \right\|^2 \leq \tau \sum_{c=0}^{\tau-1} \left\| \mathbf{g}_j^{(c,r)} \right\|^2 \tag{8}$$

655 where the last inequality is due to  $\left\|\sum_{j=1}^n \mathbf{a}_i\right\|^2 \leq n \sum_{j=1}^n \|\mathbf{a}_i\|^2$ , which together with (7) leads to  
 656 the following bound:

$$\mathbb{E}_{\xi^{(r)}|\mathbf{w}^{(r)}} \mathbb{E}_{\mathbf{S}} \left[ \left\| \frac{1}{k} \sum_{j \in \mathcal{K}} \mathbf{S} \left( \sum_{c=0}^{\tau-1} \tilde{\mathbf{g}}_j^{(c,r)} \right) \right\|^2 \right] \leq (\omega + 1) \frac{\tau \sigma^2}{k} + \tau \left( \frac{\omega}{k} + 1 \right) \sum_{j=1}^p q_j \|\mathbf{g}_j^{(c,r)}\|^2, \quad (9)$$

657 and the proof is complete.  $\square$

658 **Lemma 2.** *Under Assumption 1, and according to the FedCOM algorithm the expected inner product*  
 659 *between stochastic gradient and full batch gradient can be bounded with:*

$$-\mathbb{E}_{\xi, \mathbf{S}, \mathcal{K}} \left[ \left\langle \nabla f(\mathbf{w}^{(r)}), \tilde{\mathbf{g}}^{(r)} \right\rangle \right] \leq \frac{1}{2} \eta \frac{1}{m} \sum_{j=1}^m \sum_{c=0}^{\tau-1} \left[ -\|\nabla f(\mathbf{w}^{(r)})\|_2^2 - \|\nabla f(\mathbf{w}_j^{(c,r)})\|_2^2 + L^2 \|\mathbf{w}^{(r)} - \mathbf{w}_j^{(c,r)}\|_2^2 \right] \quad (10)$$

660 *Proof.* We have:

$$\begin{aligned} & -\mathbb{E}_{\{\xi_1^{(t)}, \dots, \xi_m^{(t)} | \mathbf{w}_1^{(t)}, \dots, \mathbf{w}_m^{(t)}\}} \mathbb{E}_{\mathbf{S}, \mathcal{K}} \left[ \left\langle \nabla f(\mathbf{w}^{(r)}), \tilde{\mathbf{g}}_{\mathbf{S}, \mathcal{K}}^{(r)} \right\rangle \right] \\ &= -\mathbb{E}_{\{\xi_1^{(t)}, \dots, \xi_m^{(t)} | \mathbf{w}_1^{(t)}, \dots, \mathbf{w}_m^{(t)}\}} \left[ \left\langle \nabla f(\mathbf{w}^{(r)}), \eta \sum_{j \in \mathcal{K}} q_j \sum_{c=0}^{\tau-1} \tilde{\mathbf{g}}_j^{(c,r)} \right\rangle \right] \\ &= -\left\langle \nabla f(\mathbf{w}^{(r)}), \eta \sum_{j=1}^m q_j \sum_{c=0}^{\tau-1} \mathbb{E}_{\xi, \mathbf{S}} \left[ \tilde{\mathbf{g}}_{j, \mathbf{S}}^{(c,r)} \right] \right\rangle \\ &= -\eta \sum_{c=0}^{\tau-1} \sum_{j=1}^m q_j \left\langle \nabla f(\mathbf{w}^{(r)}), \mathbf{g}_j^{(c,r)} \right\rangle \\ &\stackrel{\textcircled{1}}{=} \frac{1}{2} \eta \sum_{c=0}^{\tau-1} \sum_{j=1}^m q_j \left[ -\|\nabla f(\mathbf{w}^{(r)})\|_2^2 - \|\nabla f(\mathbf{w}_j^{(c,r)})\|_2^2 + \|\nabla f(\mathbf{w}^{(r)}) - \nabla f(\mathbf{w}_j^{(c,r)})\|_2^2 \right] \\ &\stackrel{\textcircled{2}}{\leq} \frac{1}{2} \eta \sum_{c=0}^{\tau-1} \sum_{j=1}^m q_j \left[ -\|\nabla f(\mathbf{w}^{(r)})\|_2^2 - \|\nabla f(\mathbf{w}_j^{(c,r)})\|_2^2 + L^2 \|\mathbf{w}^{(r)} - \mathbf{w}_j^{(c,r)}\|_2^2 \right] \end{aligned} \quad (11)$$

661 where ① is due to  $2\langle \mathbf{a}, \mathbf{b} \rangle = \|\mathbf{a}\|^2 + \|\mathbf{b}\|^2 - \|\mathbf{a} - \mathbf{b}\|^2$ , and ② follows from Assumption 1.  $\square$

662 The following lemma bounds the distance of local solutions from global solution at  $r$ th communication  
 663 round.

664 **Lemma 3.** *Under Assumptions 2 we have:*

$$\mathbb{E} \left[ \|\mathbf{w}^{(r)} - \mathbf{w}_j^{(c,r)}\|_2^2 \right] \leq \eta^2 \tau \sum_{c=0}^{\tau-1} \left\| \mathbf{g}_j^{(c,r)} \right\|_2^2 + \eta^2 \tau \sigma^2$$

665 *Proof.* Note that

$$\begin{aligned} \mathbb{E} \left[ \left\| \mathbf{w}^{(r)} - \mathbf{w}_j^{(c,r)} \right\|_2^2 \right] &= \mathbb{E} \left[ \left\| \mathbf{w}^{(r)} - \left( \mathbf{w}^{(r)} - \eta \sum_{k=0}^c \tilde{\mathbf{g}}_j^{(k,r)} \right) \right\|_2^2 \right] \\ &= \mathbb{E} \left[ \left\| \eta \sum_{k=0}^c \tilde{\mathbf{g}}_j^{(k,r)} \right\|_2^2 \right] \\ &\stackrel{\textcircled{1}}{=} \mathbb{E} \left[ \left\| \eta \sum_{k=0}^c \left( \tilde{\mathbf{g}}_j^{(k,r)} - \mathbf{g}_j^{(k,r)} \right) \right\|_2^2 \right] + \mathbb{E} \left[ \left\| \eta \sum_{k=0}^c \mathbf{g}_j^{(k,r)} \right\|_2^2 \right] \end{aligned}$$

$$\begin{aligned}
& \stackrel{\textcircled{2}}{=} \eta^2 \sum_{k=0}^c \mathbb{E} \left[ \left\| \left( \tilde{\mathbf{g}}_j^{(k,r)} - \mathbf{g}_j^{(k,r)} \right) \right\|_2^2 \right] + (c+1) \eta^2 \sum_{k=0}^c \left[ \left\| \mathbf{g}_j^{(k,r)} \right\|_2^2 \right] \\
& \leq \eta^2 \sum_{k=0}^{\tau-1} \mathbb{E} \left[ \left\| \left( \tilde{\mathbf{g}}_j^{(k,r)} - \mathbf{g}_j^{(k,r)} \right) \right\|_2^2 \right] + \tau \eta^2 \sum_{k=0}^{\tau-1} \left[ \left\| \mathbf{g}_j^{(k,r)} \right\|_2^2 \right] \\
& \stackrel{\textcircled{3}}{\leq} \eta^2 \sum_{k=0}^{\tau-1} \sigma^2 + \tau \eta^2 \sum_{k=0}^{\tau-1} \left[ \left\| \mathbf{g}_j^{(k,r)} \right\|_2^2 \right] \\
& = \eta^2 \tau \sigma^2 + \eta^2 \sum_{k=0}^{\tau-1} \tau \left\| \mathbf{g}_j^{(k,r)} \right\|_2^2
\end{aligned} \tag{12}$$

666 where ① comes from  $\mathbb{E}[\mathbf{x}^2] = \text{Var}[\mathbf{x}] + [\mathbb{E}[\mathbf{x}]]^2$  and ② holds because  $\text{Var}\left(\sum_{j=1}^n \mathbf{x}_j\right) =$   
667  $\sum_{j=1}^n \text{Var}(\mathbf{x}_j)$  for i.i.d. vectors  $\mathbf{x}_i$  (and i.i.d. assumption comes from i.i.d. sampling), and fi-  
668 nally ③ follows from Assumption 2.  $\square$

### 669 C.1.1 Main result for the non-convex setting

670 Now we are ready to present our result for the homogeneous setting. We first state and prove the  
671 result for the general non-convex objectives.

672 **Theorem 4** (non-convex). *For FedSKETCH( $\tau, \eta, \gamma$ ), for all  $0 \leq t \leq R\tau - 1$ , under Assumptions 1*  
673 *to 2, if the learning rate satisfies*

$$1 \geq \tau^2 L^2 \eta^2 + \left(\frac{\omega}{k} + 1\right) \eta \gamma L \tau \tag{13}$$

674 *and all local model parameters are initialized at the same point  $\mathbf{w}^{(0)}$ , then the average-squared*  
675 *gradient after  $\tau$  iterations is bounded as follows:*

$$\frac{1}{R} \sum_{r=0}^{R-1} \left\| \nabla f(\mathbf{w}^{(r)}) \right\|_2^2 \leq \frac{2(f(\mathbf{w}^{(0)}) - f(\mathbf{w}^{(*)}))}{\eta \gamma \tau R} + \frac{L \eta \gamma (\omega + 1)}{k} \sigma^2 + L^2 \eta^2 \tau \sigma^2, \tag{14}$$

676 *where  $\mathbf{w}^{(*)}$  is the global optimal solution with function value  $f(\mathbf{w}^{(*)})$ .*

677 *Proof.* Before proceeding with the proof of Theorem 4, we would like to highlight that

$$\mathbf{w}^{(r)} - \mathbf{w}_j^{(\tau,r)} = \eta \sum_{c=0}^{\tau-1} \tilde{\mathbf{g}}_j^{(c,r)}. \tag{15}$$

678 From the updating rule of Algorithm 3 we have

$$\mathbf{w}^{(r+1)} = \mathbf{w}^{(r)} - \gamma \eta \left( \frac{1}{k} \sum_{j \in \mathcal{K}} \mathbf{S} \left( \sum_{c=0, r}^{\tau-1} \tilde{\mathbf{g}}_j^{(c,r)} \right) \right) = \mathbf{w}^{(r)} - \gamma \left[ \frac{\eta}{k} \sum_{j \in \mathcal{K}} \mathbf{S} \left( \sum_{c=0}^{\tau-1} \tilde{\mathbf{g}}_j^{(c,r)} \right) \right].$$

In what follows, we use the following notation to denote the stochastic gradient used to update the global model at  $r$ th communication round

$$\tilde{\mathbf{g}}_{\mathbf{S}, \mathcal{K}}^{(r)} \triangleq \frac{\eta}{p} \sum_{j=1}^p \mathbf{S} \left( \frac{\mathbf{w}^{(r)} - \mathbf{w}_j^{(\tau,r)}}{\eta} \right) = \frac{1}{k} \sum_{j \in \mathcal{K}} \mathbf{S} \left( \sum_{c=0}^{\tau-1} \tilde{\mathbf{g}}_j^{(c,r)} \right).$$

679 and notice that  $\mathbf{w}^{(r)} = \mathbf{w}^{(r-1)} - \gamma \tilde{\mathbf{g}}^{(r)}$ .

680 Then using the unbiased estimation property of sketching we have:

$$\mathbb{E}_{\mathbf{S}} \left[ \tilde{\mathbf{g}}_{\mathbf{S}}^{(r)} \right] = \frac{1}{k} \sum_{j \in \mathcal{K}} \left[ -\eta \mathbb{E}_{\mathbf{S}} \left[ \mathbf{S} \left( \sum_{c=0}^{\tau-1} \tilde{\mathbf{g}}_j^{(c,r)} \right) \right] \right] = \frac{1}{k} \sum_{j \in \mathcal{K}} \left[ -\eta \left( \sum_{c=0}^{\tau-1} \tilde{\mathbf{g}}_j^{(c,r)} \right) \right] \triangleq \tilde{\mathbf{g}}_{\mathbf{S}, \mathcal{K}}^{(r)}.$$

681 From the  $L$ -smoothness gradient assumption on global objective, by using  $\tilde{\mathbf{g}}^{(r)}$  in inequality (15) we  
 682 have:

$$f(\mathbf{w}^{(r+1)}) - f(\mathbf{w}^{(r)}) \leq -\gamma \langle \nabla f(\mathbf{w}^{(r)}), \tilde{\mathbf{g}}^{(r)} \rangle + \frac{\gamma^2 L}{2} \|\tilde{\mathbf{g}}^{(r)}\|^2 \quad (16)$$

683 By taking expectation on both sides of above inequality over sampling, we get:

$$\begin{aligned} \mathbb{E} \left[ \mathbb{E}_{\mathbf{S}} \left[ f(\mathbf{w}^{(r+1)}) - f(\mathbf{w}^{(r)}) \right] \right] &\leq -\gamma \mathbb{E} \left[ \mathbb{E}_{\mathbf{S}} \left[ \langle \nabla f(\mathbf{w}^{(r)}), \tilde{\mathbf{g}}_{\mathbf{S}}^{(r)} \rangle \right] \right] + \frac{\gamma^2 L}{2} \mathbb{E} \left[ \mathbb{E}_{\mathbf{S}} \|\tilde{\mathbf{g}}_{\mathbf{S}}^{(r)}\|^2 \right] \\ &\stackrel{(a)}{=} -\gamma \underbrace{\mathbb{E} \left[ \langle \nabla f(\mathbf{w}^{(r)}), \tilde{\mathbf{g}}^{(r)} \rangle \right]}_{(I)} + \frac{\gamma^2 L}{2} \underbrace{\mathbb{E} \left[ \mathbb{E}_{\mathbf{S}} \left[ \|\tilde{\mathbf{g}}_{\mathbf{S}}^{(r)}\|^2 \right] \right]}_{(II)}. \end{aligned} \quad (17)$$

684 We proceed to use Lemma 1, Lemma 2, and Lemma 3, to bound terms (I) and (II) in right hand side  
 685 of (17), which gives

$$\begin{aligned} &\mathbb{E} \left[ \mathbb{E}_{\mathbf{S}} \left[ f(\mathbf{w}^{(r+1)}) - f(\mathbf{w}^{(r)}) \right] \right] \\ &\leq \gamma \frac{1}{2} \eta \sum_{j=1}^p q_j \sum_{c=0}^{\tau-1} \left[ -\left\| \nabla f(\mathbf{w}^{(r)}) \right\|_2^2 - \left\| \mathbf{g}_j^{(c,r)} \right\|_2^2 + L^2 \eta^2 \sum_{c=0}^{\tau-1} \left[ \tau \left\| \mathbf{g}_j^{(c,r)} \right\|_2^2 + \sigma^2 \right] \right] \\ &\quad + \frac{\gamma^2 L (\frac{\omega}{k} + 1)}{2} \left[ \eta^2 \tau \sum_{j=1}^p q_j \sum_{c=0}^{\tau-1} \left\| \mathbf{g}_j^{(c,r)} \right\|_2^2 \right] + \frac{\gamma^2 \eta^2 L (\omega + 1)}{2} \frac{\tau \sigma^2}{k} \\ &\stackrel{\textcircled{1}}{\leq} \frac{\gamma \eta}{2} \sum_{j=1}^p q_j \sum_{c=0}^{\tau-1} \left[ -\left\| \nabla f(\mathbf{w}^{(r)}) \right\|_2^2 - \left\| \mathbf{g}_j^{(c,r)} \right\|_2^2 + \tau L^2 \eta^2 \left[ \tau \left\| \mathbf{g}_j^{(c,r)} \right\|_2^2 + \sigma^2 \right] \right] \\ &\quad + \frac{\gamma^2 L (\frac{\omega}{k} + 1)}{2} \left[ \eta^2 \tau \sum_{j=1}^p q_j \sum_{c=0}^{\tau-1} \left\| \mathbf{g}_j^{(c,r)} \right\|_2^2 \right] + \frac{\gamma^2 \eta^2 L (\omega + 1)}{2} \frac{\tau \sigma^2}{k} \\ &= -\eta \gamma \frac{\tau}{2} \left\| \nabla f(\mathbf{w}^{(r)}) \right\|_2^2 \\ &\quad - \left( 1 - \tau L^2 \eta^2 \tau - \left( \frac{\omega}{k} + 1 \right) \eta \gamma L \tau \right) \frac{\eta \gamma}{2} \sum_{j=1}^p q_j \sum_{c=0}^{\tau-1} \left\| \mathbf{g}_j^{(c,r)} \right\|_2^2 + \frac{L \tau \gamma \eta^2}{2k} (k L \tau \eta + \gamma (\omega + 1)) \sigma^2 \\ &\stackrel{\textcircled{2}}{\leq} -\eta \gamma \frac{\tau}{2} \left\| \nabla f(\mathbf{w}^{(r)}) \right\|_2^2 + \frac{L \tau \gamma \eta^2}{2k} (k L \tau \eta + \gamma (\omega + 1)) \sigma^2, \end{aligned} \quad (18)$$

686 where in ① we incorporate outer summation  $\sum_{c=0}^{\tau-1}$ , and ② follows from condition

$$1 \geq \tau L^2 \eta^2 \tau + \left( \frac{\omega}{k} + 1 \right) \eta \gamma L \tau.$$

687 Summing up for all  $R$  communication rounds and rearranging the terms gives:

$$\frac{1}{R} \sum_{r=0}^{R-1} \left\| \nabla f(\mathbf{w}^{(r)}) \right\|_2^2 \leq \frac{2 (f(\mathbf{w}^{(0)}) - f(\mathbf{w}^{(*)}))}{\eta \gamma \tau R} + \frac{L \eta \gamma (\omega + 1)}{k} \sigma^2 + L^2 \eta^2 \tau \sigma^2.$$

688 From the above inequality, is it easy to see that in order to achieve a linear speed up, we need to have

689  $\eta \gamma = O\left(\frac{\sqrt{k}}{\sqrt{R\tau}}\right).$  □

690 **Corollary 3** (Linear speed up). *In (14) for the choice of  $\eta \gamma = O\left(\frac{1}{L} \sqrt{\frac{k}{R\tau(\omega+1)}}\right)$ , and  $\gamma \geq k$  the*  
 691 *convergence rate reduces to:*

$$\frac{1}{R} \sum_{r=0}^{R-1} \left\| \nabla f(\mathbf{w}^{(r)}) \right\|_2^2 \leq O \left( \frac{L \sqrt{(\omega+1)} (f(\mathbf{w}^{(0)}) - f(\mathbf{w}^{*}))}{\sqrt{k R \tau}} + \frac{\left( \sqrt{(\omega+1)} \right) \sigma^2}{\sqrt{k R \tau}} + \frac{k \sigma^2}{R \gamma^2} \right). \quad (19)$$



692 Note that according to (19), if we pick a fixed constant value for  $\gamma$ , in order to achieve an  $\epsilon$ -accurate  
693 solution,  $R = O\left(\frac{1}{\epsilon}\right)$  communication rounds and  $\tau = O\left(\frac{\omega+1}{k\epsilon}\right)$  local updates are necessary. We  
694 also highlight that (19) also allows us to choose  $R = O\left(\frac{\omega+1}{\epsilon}\right)$  and  $\tau = O\left(\frac{1}{k\epsilon}\right)$  to get the same  
695 convergence rate.

696 **Remark 3.** Condition in (13) can be rewritten as

$$\begin{aligned}\eta &\leq \frac{-\gamma L\tau \left(\frac{\omega}{k} + 1\right) + \sqrt{\gamma^2 \left(L\tau \left(\frac{\omega}{k} + 1\right)\right)^2 + 4L^2\tau^2}}{2L^2\tau^2} \\ &= \frac{-\gamma L\tau \left(\frac{\omega}{k} + 1\right) + L\tau \sqrt{\left(\frac{\omega}{k} + 1\right)^2 \gamma^2 + 4}}{2L^2\tau^2} \\ &= \frac{\sqrt{\left(\frac{\omega}{k} + 1\right)^2 \gamma^2 + 4} - \left(\frac{\omega}{k} + 1\right) \gamma}{2L\tau}.\end{aligned}\quad (20)$$

697 So based on (20), if we set  $\eta = O\left(\frac{1}{L\gamma} \sqrt{\frac{k}{R\tau(\omega+1)}}\right)$ , it implies that:

$$R \geq \frac{\tau k}{(\omega + 1) \gamma^2 \left( \sqrt{\left(\frac{\omega}{k} + 1\right)^2 \gamma^2 + 4} - \left(\frac{\omega}{k} + 1\right) \gamma \right)^2}.\quad (21)$$

698 We note that  $\gamma^2 \left( \sqrt{\left(\frac{\omega}{k} + 1\right)^2 \gamma^2 + 4} - \left(\frac{\omega}{k} + 1\right) \gamma \right)^2 = \Theta(1) \leq 5$  therefore even for  $\gamma \geq m$  we  
699 need to have

$$R \geq \frac{\tau k}{5(\omega + 1)} = O\left(\frac{\tau k}{(\omega + 1)}\right).\quad (22)$$

700 Therefore, for the choice of  $\tau = O\left(\frac{\omega+1}{k\epsilon}\right)$ , due to condition in (22), we need to have  $R = O\left(\frac{1}{\epsilon}\right)$ .  
701 Similarly, we can have  $R = O\left(\frac{\omega+1}{\epsilon}\right)$  and  $\tau = O\left(\frac{1}{k\epsilon}\right)$ .

702 **Corollary 4** (Special case,  $\gamma = 1$ ). By letting  $\gamma = 1$ ,  $\omega = 0$  and  $k = p$  the convergence rate in (14)  
703 reduces to

$$\frac{1}{R} \sum_{r=0}^{R-1} \left\| \nabla f(\mathbf{w}^{(r)}) \right\|_2^2 \leq \frac{2(f(\mathbf{w}^{(0)}) - f(\mathbf{w}^{(*)}))}{\eta R \tau} + \frac{L\eta}{p} \sigma^2 + L^2 \eta^2 \tau \sigma^2,$$

704 which matches the rate obtained in [43]. In this case the communication complexity and the number  
705 of local updates become

$$R = O\left(\frac{p}{\epsilon}\right), \quad \tau = O\left(\frac{1}{\epsilon}\right),$$

706 which simply implies that in this special case the convergence rate of our algorithm reduces to the  
707 rate obtained in [43], which indicates the tightness of our analysis.

### 708 C.1.2 Main result for the PL/Strongly convex setting

709 We now turn to stating the convergence rate for the homogeneous setting under PL condition which  
710 naturally leads to the same rate for strongly convex functions.

711 **Theorem 5** (PL or strongly convex). For  $\text{FedSKETCH}(\tau, \eta, \gamma)$ , for all  $0 \leq t \leq R\tau - 1$ , under  
712 Assumptions 1 to 2 and 3, if the learning rate satisfies

$$1 \geq \tau^2 L^2 \eta^2 + \left(\frac{\omega}{k} + 1\right) \eta \gamma L \tau$$

713 and if the all the models are initialized with  $\mathbf{w}^{(0)}$  we obtain:

$$\mathbb{E} \left[ f(\mathbf{w}^{(R)}) - f(\mathbf{w}^{(*)}) \right] \leq (1 - \eta \gamma \mu \tau)^R \left( f(\mathbf{w}^{(0)}) - f(\mathbf{w}^{(*)}) \right) + \frac{1}{\mu} \left[ \frac{1}{2} L^2 \tau \eta^2 \sigma^2 + (1 + \omega) \frac{\gamma \eta L \sigma^2}{2k} \right]$$

714 *Proof.* From (18) under condition:

$$1 \geq \tau L^2 \eta^2 \tau + \left(\frac{\omega}{k} + 1\right) \eta \gamma L \tau$$

715 we obtain:

$$\begin{aligned} \mathbb{E} \left[ f(\mathbf{w}^{(r+1)}) - f(\mathbf{w}^{(r)}) \right] &\leq -\eta \gamma \frac{\tau}{2} \left\| \nabla f(\mathbf{w}^{(r)}) \right\|_2^2 + \frac{L \tau \gamma \eta^2}{2k} (k L \tau \eta + \gamma(\omega + 1)) \sigma^2 \\ &\leq -\eta \mu \gamma \tau \left( f(\mathbf{w}^{(r)}) - f(\mathbf{w}^{(r)}) \right) + \frac{L \tau \gamma \eta^2}{2k} (k L \tau \eta + \gamma(\omega + 1)) \sigma^2 \end{aligned} \quad (23)$$

716 which leads to the following bound:

$$\mathbb{E} \left[ f(\mathbf{w}^{(r+1)}) - f(\mathbf{w}^{(*)}) \right] \leq (1 - \eta \mu \gamma \tau) \left[ f(\mathbf{w}^{(r)}) - f(\mathbf{w}^{(*)}) \right] + \frac{L \tau \gamma \eta^2}{2k} (k L \tau \eta + (\omega + 1) \gamma) \sigma^2$$

717 By setting  $\Delta = 1 - \eta \mu \gamma \tau$  we obtain the following bound:

$$\begin{aligned} &\mathbb{E} \left[ f(\mathbf{w}^{(R)}) - f(\mathbf{w}^{(*)}) \right] \\ &\leq \Delta^R \left[ f(\mathbf{w}^{(0)}) - f(\mathbf{w}^{(*)}) \right] + \frac{1 - \Delta^R}{1 - \Delta} \frac{L \tau \gamma \eta^2}{2k} (k L \tau \eta + (\omega + 1) \gamma) \sigma^2 \\ &\leq \Delta^R \left[ f(\mathbf{w}^{(0)}) - f(\mathbf{w}^{(*)}) \right] + \frac{1}{1 - \Delta} \frac{L \tau \gamma \eta^2}{2k} (k L \tau \eta + (\omega + 1) \gamma) \sigma^2 \\ &= (1 - \eta \mu \gamma \tau)^R \left[ f(\mathbf{w}^{(0)}) - f(\mathbf{w}^{(*)}) \right] + \frac{1}{\eta \mu \gamma \tau} \frac{L \tau \gamma \eta^2}{2k} (k L \tau \eta + (\omega + 1) \gamma) \sigma^2 \end{aligned} \quad (24)$$

718  $\square$

719 **Corollary 5.** If we let  $\eta \gamma \mu \tau \leq \frac{1}{2}$ ,  $\eta = \frac{1}{2L(\frac{\omega}{k} + 1)\tau \gamma}$  and  $\kappa = \frac{L}{\mu}$  the convergence error in Theorem 5,  
720 with  $\gamma \geq k$  results in:

$$\begin{aligned} &\mathbb{E} \left[ f(\mathbf{w}^{(R)}) - f(\mathbf{w}^{(*)}) \right] \\ &\leq e^{-\eta \gamma \mu \tau R} \left( f(\mathbf{w}^{(0)}) - f(\mathbf{w}^{(*)}) \right) + \frac{1}{\mu} \left[ \frac{1}{2} \tau L^2 \eta^2 \sigma^2 + (1 + \omega) \frac{\gamma \eta L \sigma^2}{2k} \right] \\ &\leq e^{-\frac{R}{2(\frac{\omega}{k} + 1)\kappa}} \left( f(\mathbf{w}^{(0)}) - f(\mathbf{w}^{(*)}) \right) + \frac{1}{\mu} \left[ \frac{1}{2} L^2 \frac{\tau \sigma^2}{L^2 (\frac{\omega}{k} + 1)^2 \gamma^2 \tau^2} + \frac{(1 + \omega) L \sigma^2}{2 (\frac{\omega}{k} + 1) L \tau k} \right] \\ &= O \left( e^{-\frac{R}{2(\frac{\omega}{k} + 1)\kappa}} \left( f(\mathbf{w}^{(0)}) - f(\mathbf{w}^{(*)}) \right) + \frac{\sigma^2}{(\frac{\omega}{k} + 1)^2 \gamma^2 \mu \tau} + \frac{(\omega + 1) \sigma^2}{\mu (\frac{\omega}{k} + 1) \tau k} \right) \\ &= O \left( e^{-\frac{R}{2(\frac{\omega}{k} + 1)\kappa}} \left( f(\mathbf{w}^{(0)}) - f(\mathbf{w}^{(*)}) \right) + \frac{\sigma^2}{\gamma^2 \mu \tau} + \frac{(\omega + 1) \sigma^2}{\mu (\frac{\omega}{k} + 1) \tau k} \right) \end{aligned} \quad (25)$$

721 which indicates that to achieve an error of  $\epsilon$ , we need to have  $R = O \left( \left( \frac{\omega}{k} + 1 \right) \kappa \log \left( \frac{1}{\epsilon} \right) \right)$  and  $\tau =$   
722  $\frac{(\omega + 1)}{k(\frac{\omega}{k} + 1)\epsilon}$ . Additionally, we note that if  $\gamma \rightarrow \infty$ , yet  $R = O \left( \left( \frac{\omega}{k} + 1 \right) \kappa \log \left( \frac{1}{\epsilon} \right) \right)$  and  $\tau = \frac{(\omega + 1)}{k(\frac{\omega}{k} + 1)\epsilon}$   
723 will be necessary.

### 724 C.1.3 Main result for the general convex setting

725 **Theorem 6 (Convex).** For a general convex function  $f(\mathbf{w})$  with optimal solution  $\mathbf{w}^{(*)}$ , using  
726  $\text{FedSKETCH}(\tau, \eta, \gamma)$  to optimize  $\hat{f}(\mathbf{w}, \phi) = f(\mathbf{w}) + \frac{\phi}{2} \|\mathbf{w}\|^2$ , for all  $0 \leq t \leq R\tau - 1$ , under  
727 Assumptions 1 to 2, if the learning rate satisfies

$$1 \geq \tau^2 L^2 \eta^2 + \left(\frac{\omega}{k} + 1\right) \eta \gamma L \tau$$

728 and if the all the models initiate with  $\mathbf{w}^{(0)}$ , with  $\phi = \frac{1}{\sqrt{k\tau}}$  and  $\eta = \frac{1}{2L\gamma\tau(1+\frac{\omega}{k})}$  we obtain:

$$\begin{aligned} \mathbb{E}\left[f(\mathbf{w}^{(R)}) - f(\mathbf{w}^{(*)})\right] &\leq e^{-\frac{R}{2L(1+\frac{\omega}{k})\sqrt{m\tau}}} \left(f(\mathbf{w}^{(0)}) - f(\mathbf{w}^{(*)})\right) \\ &\quad + \left[\frac{\sqrt{k}\sigma^2}{8\sqrt{\tau}\gamma^2(1+\frac{\omega}{k})^2} + \frac{(\omega+1)\sigma^2}{4(\frac{\omega}{k}+1)\sqrt{k\tau}}\right] + \frac{1}{2\sqrt{k\tau}} \|\mathbf{w}^{(*)}\|^2 \end{aligned} \quad (26)$$

729 We note that above theorem implies that to achieve a convergence error of  $\epsilon$  we need to have  
 730  $R = O\left(L\left(1+\frac{\omega}{k}\right)\frac{1}{\epsilon}\log\left(\frac{1}{\epsilon}\right)\right)$  and  $\tau = O\left(\frac{(\omega+1)^2}{k(\frac{\omega}{k}+1)^2\epsilon}\right)$ .

731 *Proof.* Since  $\tilde{f}(\mathbf{w}^{(r)}, \phi) = f(\mathbf{w}^{(r)}) + \frac{\phi}{2} \|\mathbf{w}^{(r)}\|^2$  is  $\phi$ -PL, according to Theorem 5, we have:

$$\begin{aligned} &\tilde{f}(\mathbf{w}^{(R)}, \phi) - \tilde{f}(\mathbf{w}^{(*)}, \phi) \\ &= f(\mathbf{w}^{(r)}) + \frac{\phi}{2} \|\mathbf{w}^{(r)}\|^2 - \left(f(\mathbf{w}^{(*)}) + \frac{\phi}{2} \|\mathbf{w}^{(*)}\|^2\right) \\ &\leq (1 - \eta\gamma\phi\tau)^R \left(f(\mathbf{w}^{(0)}) - f(\mathbf{w}^{(*)})\right) + \frac{1}{\phi} \left[\frac{1}{2}L^2\tau\eta^2\sigma^2 + (1+\omega)\frac{\gamma\eta L\sigma^2}{2k}\right] \end{aligned} \quad (27)$$

732 Next rearranging (27) and replacing  $\mu$  with  $\phi$  leads to the following error bound:

$$\begin{aligned} &f(\mathbf{w}^{(R)}) - f^* \\ &\leq (1 - \eta\gamma\phi\tau)^R \left(f(\mathbf{w}^{(0)}) - f(\mathbf{w}^{(*)})\right) + \frac{1}{\phi} \left[\frac{1}{2}L^2\tau\eta^2\sigma^2 + (1+\omega)\frac{\gamma\eta L\sigma^2}{2k}\right] \\ &\quad + \frac{\phi}{2} \left(\|\mathbf{w}^*\|^2 - \|\mathbf{w}^{(r)}\|^2\right) \\ &\leq e^{-(\eta\gamma\phi\tau)R} \left(f(\mathbf{w}^{(0)}) - f(\mathbf{w}^{(*)})\right) + \frac{1}{\phi} \left[\frac{1}{2}L^2\tau\eta^2\sigma^2 + (1+\omega)\frac{\gamma\eta L\sigma^2}{2k}\right] + \frac{\phi}{2} \|\mathbf{w}^{(*)}\|^2 \end{aligned}$$

733 Next, if we set  $\phi = \frac{1}{\sqrt{k\tau}}$  and  $\eta = \frac{1}{2(1+\frac{\omega}{k})L\gamma\tau}$ , we obtain that

$$\begin{aligned} &f(\mathbf{w}^{(R)}) - f^* \\ &\leq e^{-\frac{R}{2(1+\frac{\omega}{k})L\sqrt{m\tau}}} \left(f(\mathbf{w}^{(0)}) - f(\mathbf{w}^{(*)})\right) + \sqrt{k\tau} \left[\frac{\sigma^2}{8\tau\gamma^2(1+\frac{\omega}{k})^2} + \frac{(\omega+1)\sigma^2}{4(\frac{\omega}{k}+1)\tau k}\right] + \frac{1}{2\sqrt{k\tau}} \|\mathbf{w}^{(*)}\|^2, \end{aligned}$$

734 thus the proof is complete.  $\square$

## C.2 Proof of Theorem 2

The proof of Theorem 2 follows directly from the results in [13]. We first mention the general Theorem 7 from [13] for general compression noise  $\omega$ . Next, since the sketching PRIVIX and HEAPRIX, satisfy Assumption 4 with  $\omega = c \frac{d}{m}$  and  $\omega = c \frac{d}{m} - 1$  respectively with probability  $1 - \frac{\delta}{R}$  per communication round, all the results in Theorem 2, conclude from Theorem 7 with probability  $1 - \delta$  (by taking union over the all probabilities of each communication rounds with probability  $1 - \delta/R$ ) and plugging  $\omega = c \frac{d}{m}$  and  $\omega = c \frac{d}{m} - 1$  respectively into the corresponding convergence bounds. For the heterogeneous setting, the results in [13] requires the following extra assumption that naturally holds for the sketching:

**Assumption 5** ([13]). *The compression scheme  $Q$  for the heterogeneous data distribution setting satisfies the following condition  $\mathbb{E}_Q[\|\frac{1}{m} \sum_{j=1}^m Q(\mathbf{x}_j)\|^2 - \|Q(\frac{1}{m} \sum_{j=1}^m \mathbf{x}_j)\|^2] \leq G_q$ .*

We note that since sketching is a linear compressor, in the case of our algorithms for heterogeneous setting we have  $G_q = 0$ .

Next, we restate the Theorem in [13] here as follows:

**Theorem 7.** *Consider FedCOMGATE in [13]. If Assumptions 1, 3, 4 and 5 hold, then even for the case the local data distribution of users are different (heterogeneous setting) we have*

- **non-convex:** By choosing stepsizes as  $\eta = \frac{1}{L\gamma} \sqrt{\frac{p}{R\tau(\omega+1)}}$  and  $\gamma \geq p$ , we obtain that the iterates satisfy  $\frac{1}{R} \sum_{r=0}^{R-1} \|\nabla f(\mathbf{w}^{(r)})\|_2^2 \leq \epsilon$  if we set  $R = O\left(\frac{\omega+1}{\epsilon}\right)$  and  $\tau = O\left(\frac{1}{p\epsilon}\right)$ .
- **Strongly convex or PL:** By choosing stepsizes as  $\eta = \frac{1}{2L(\frac{\omega}{p}+1)\tau\gamma}$  and  $\gamma \geq \sqrt{p\tau}$ , we obtain that the iterates satisfy  $\mathbb{E}\left[f(\mathbf{w}^{(R)}) - f(\mathbf{w}^{(*)})\right] \leq \epsilon$  if we set  $R = O\left((\omega+1)\kappa \log\left(\frac{1}{\epsilon}\right)\right)$  and  $\tau = O\left(\frac{1}{p\epsilon}\right)$ .
- **Convex:** By choosing stepsizes as  $\eta = \frac{1}{2L(\omega+1)\tau\gamma}$  and  $\gamma \geq \sqrt{p\tau}$ , we obtain that the iterates satisfy  $\mathbb{E}\left[f(\mathbf{w}^{(R)}) - f(\mathbf{w}^{(*)})\right] \leq \epsilon$  if we set  $R = O\left(\frac{L(1+\omega)}{\epsilon} \log\left(\frac{1}{\epsilon}\right)\right)$  and  $\tau = O\left(\frac{1}{p\epsilon^2}\right)$ .

*Proof.* Since the sketching methods PRIVIX and HEAPRIX, satisfy the Assumption 4 with  $\omega = c \frac{d}{m}$  and  $\omega = c \frac{d}{m} - 1$  respectively with probability  $1 - \frac{\delta}{R}$  per communication round, we conclude the proofs of Theorem 2 using Theorem 7 with probability  $1 - \delta$  (by taking union over all communication rounds) and plugging  $\omega = c \frac{d}{m}$  and  $\omega = c \frac{d}{m} - 1$  respectively into the convergence bounds.  $\square$

## D Numerical Experiments and Additional Results

### D.1 Implementation of FetchSGD

Our implementation of FetchSGD basically follows the original paper (Algorithm 1 in [37]). The only difference is that, in the original algorithm, the local workers compress the gradient (in every local step) and transmit it to the central server. In our setting, we extend to the case with multiple local updates, where the difference in local weights are transmitted (same as the standard FL framework). Also, TopK compression is used to decode the sketches at the central server. We apply the same implementation trick that when accumulating the errors, we only count the non-zero coordinates and leave other coordinates zero for the accumulator. This greatly improves the empirical performance.

## 771 D.2 Additional Plots for the MNIST Experiments

### 772 D.2.1 Homogeneous setting

773 In the homogeneous case, each node has same data distribution. To achieve this setting, we randomly  
 774 choose samples uniformly from 10 classes of hand-written digits. The train loss and test accuracy  
 775 are provided in Figure 3, where we report local epochs  $\tau = 2$  in addition to the main context (single  
 776 local update). The number of users is set to 50, and in each round of training we randomly pick half  
 777 of the nodes to be active (i.e., receiving data and performing local updates). We can draw similar  
 778 conclusion: FS-HEAPRIX consistently performs better than other competing methods. The test  
 779 accuracy increases with larger  $\tau$  in homogeneous setting.

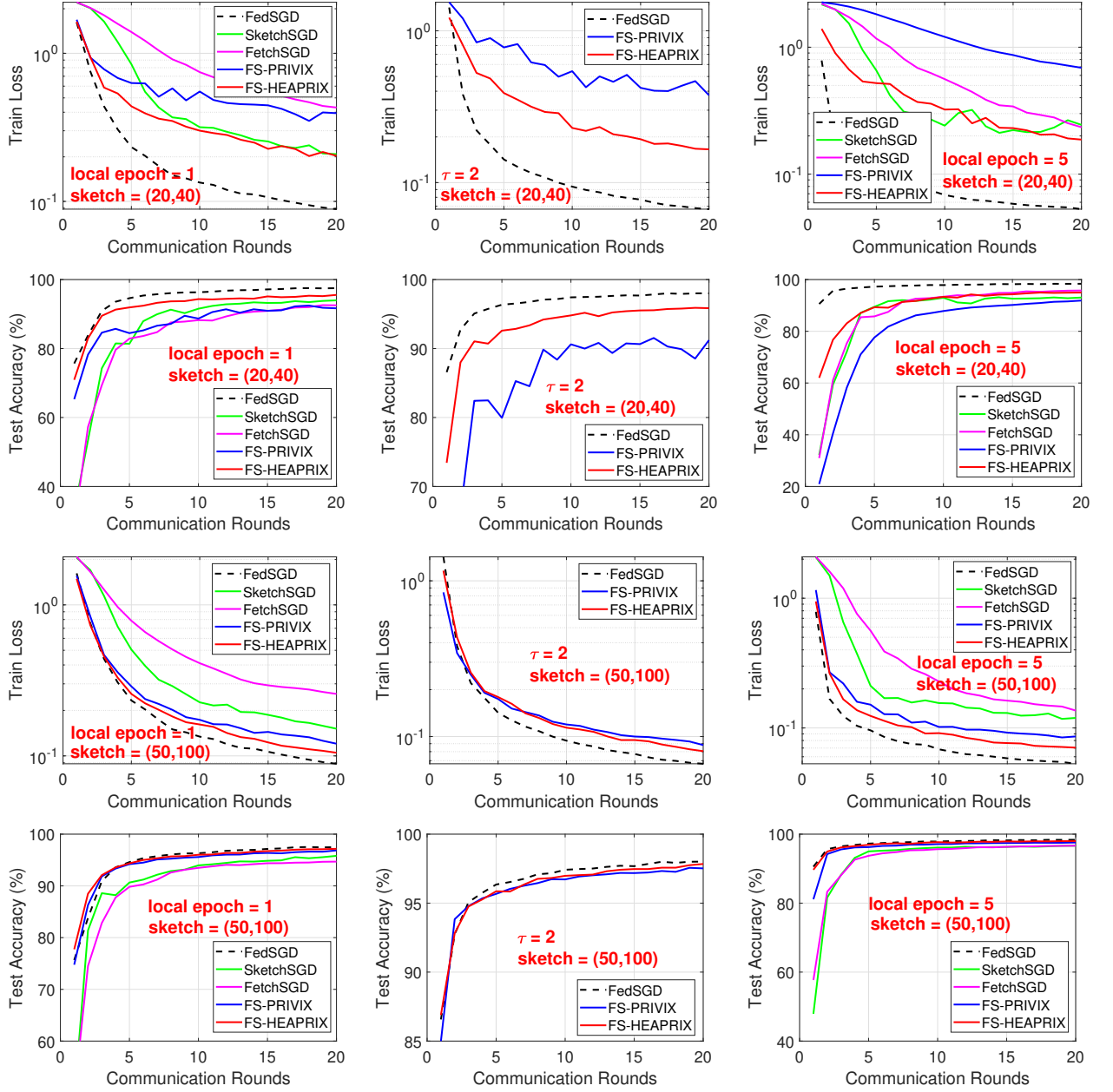


Figure 3: MNIST Homogeneous case: Comparison of compressed optimization methods on LeNet CNN architecture.

## 780 D.2.2 Heterogeneous setting

781 Analogously, we present experiments on MNIST dataset under heterogeneous data distribution,  
 782 including  $\tau = 2$ . We simulate the setting by only sending samples from one digit to each local  
 783 worker (very few nodes get two classes). We see from Figure 4 that FS-HEAPRIX shows consistent  
 784 advantage over competing methods. SketchedSGD performs poorly in this case.

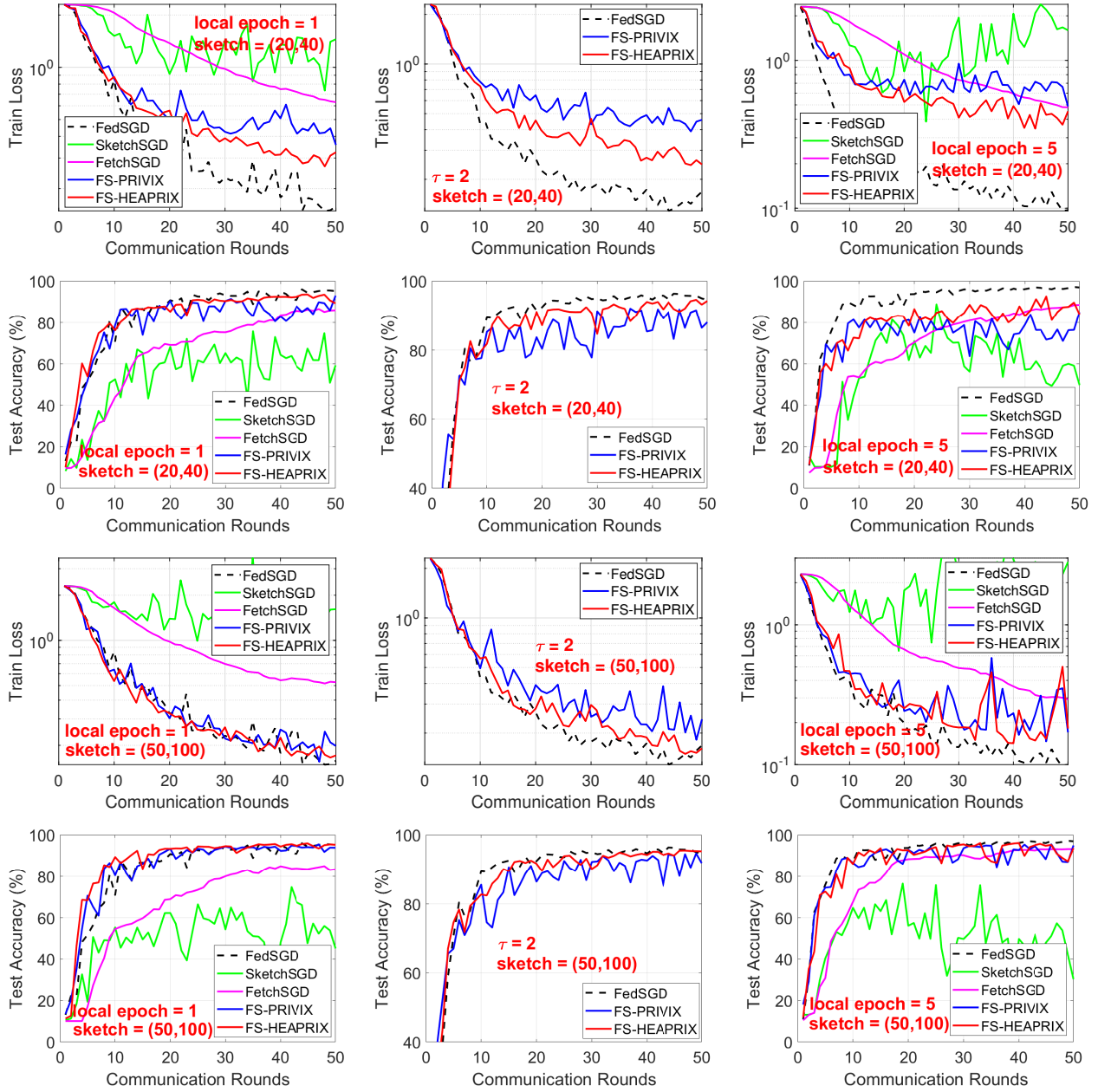


Figure 4: MNIST Heterogeneous case: Comparison of compressed optimization algorithms on LeNet CNN architecture.

### 785 D.3 Additional Experiments: CIFAR-10

786 We conduct similar sets of experiments on CIFAR10 dataset. We also use the simple LeNet CNN  
 787 structure, as in practice small models are more favorable in federated learning, due to the limitation of  
 788 mobile devices. The test accuracy is presented in Figure 5 and Figure 6, for respectively homogeneous  
 789 and heterogeneous data distribution. In general, we retrieve similar information as from MNIST  
 790 experiments: our proposed FS-HEAPRIX improves FS-PRIVIX and SketchedSGD in all cases. We  
 791 note that although the test accuracy provided by LeNet cannot reach the state-of-the-art accuracy  
 792 given by some huge models, it is also informative in terms of comparing the relative performance of  
 793 different sketching methods.

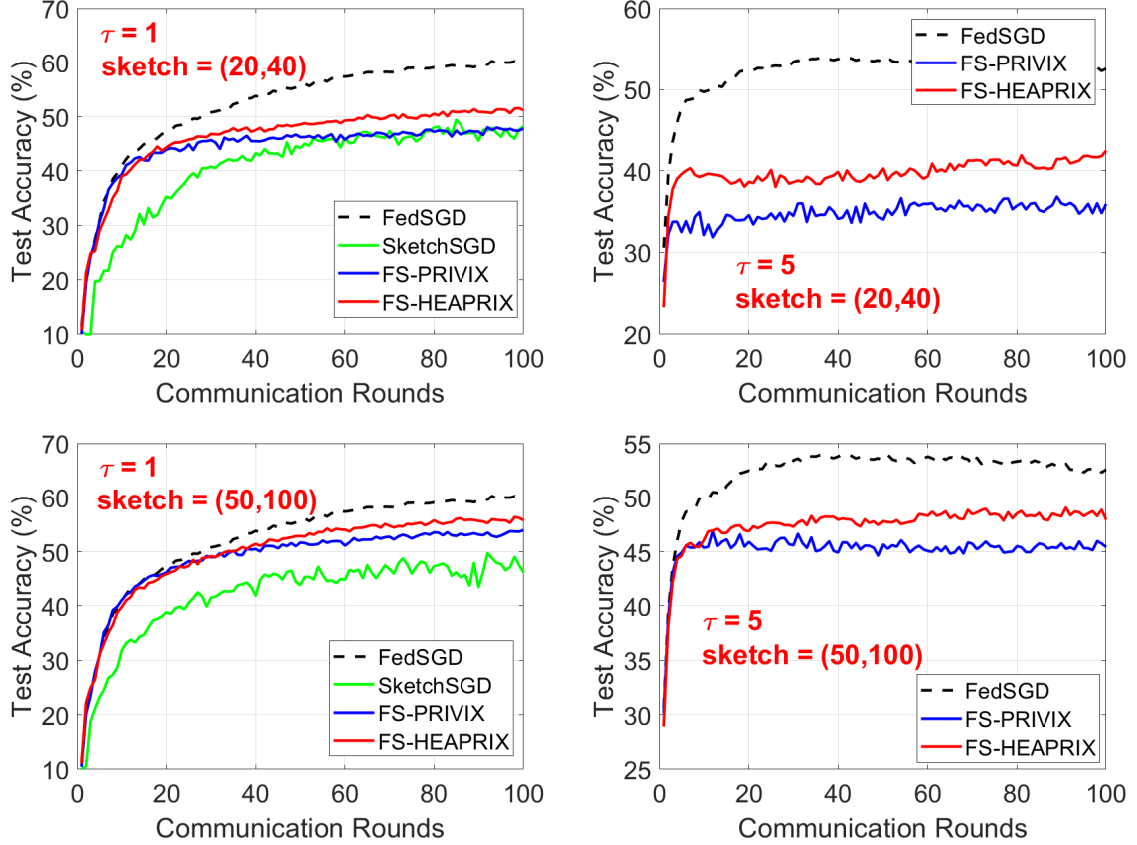


Figure 5: Homogeneous case: CIFAR10: Comparison of compressed optimization methods on LeNet CNN.



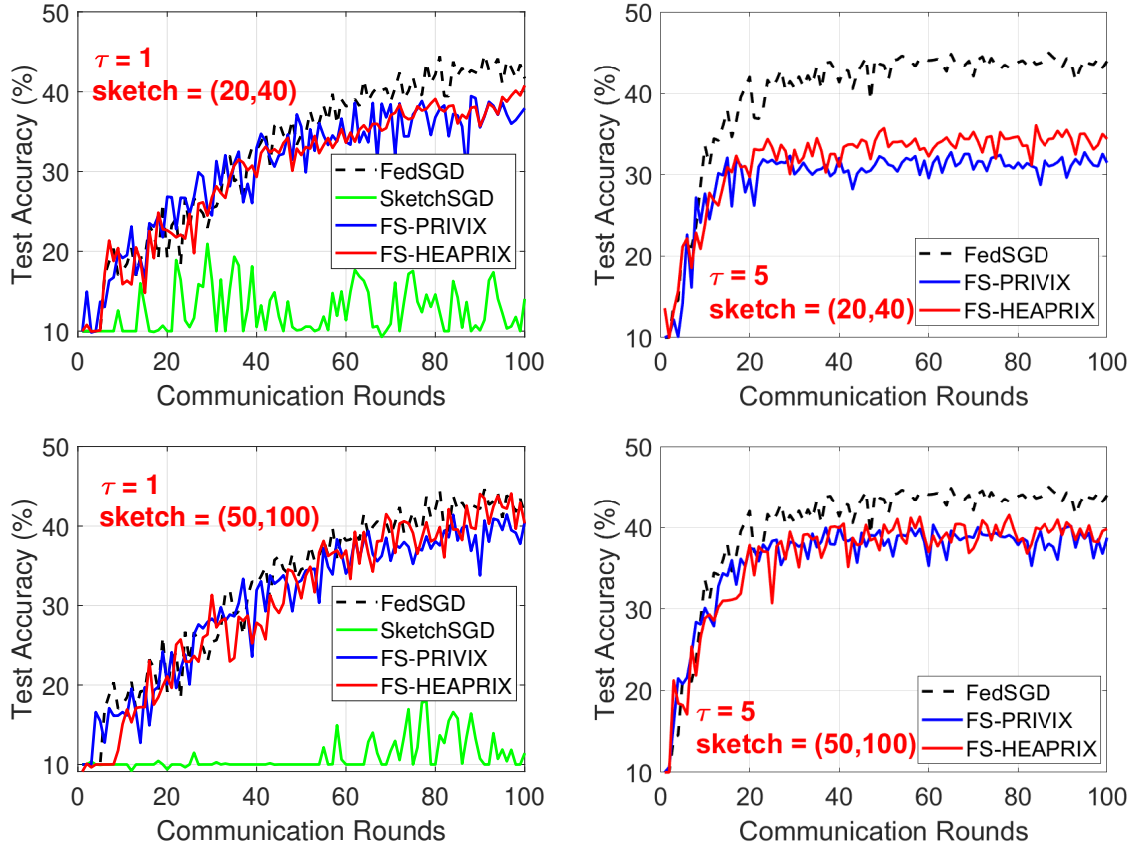


Figure 6: Heterogeneous case: CIFAR10: Comparison of compressed optimization methods on LeNet CNN.